Electric Sail Mission Analysis for Outer Solar System Exploration

Alessandro A. Quarta[*] and Giovanni Mengali[†]

University of Pisa, I-56122 Pisa, Italy

Abstract

Missions towards the boundaries of the Solar System require long transfer times and advanced propulsion systems. An interesting option is offered by electric sails, a new propulsion concept that uses the solar wind dynamic pressure for generating a continuous thrust without the need for reaction mass. The aim of this paper is to investigate the performance of such a propulsion system for obtaining escape conditions from the Solar System and planning a mission to reach the heliosphere boundaries. The problem is studied in an optimal framework, by minimizing the time to reach a given solar distance or a given hyperbolic excess speed. Depending on the value of the sail characteristic acceleration, it is possible that, in an initial mission phase, the sailcraft may approach the Sun to exploit the increased available thrust due to the growing solar wind electron density. The corresponding optimal trajectory is constrained to not pass inside a heliocentric sphere whose admissible radius is established by thermal constraints. Once the escape condition is met, the sail is jettisoned and the payload alone continues its journey without any propulsion system. A medium performance electric sail is shown to have the potentialities to reach the heliosheath, at a distance of 100 AU, in about fifteen years. Finally, the Interstellar Heliopause Probe mission is used as a reference mission to further quantify the electric sail capabilities for an optimal transfer towards the heliopause nose (200 AU).

Nomenclature

a	=	initial orbit semimajor axis
$\boldsymbol{a}_p$	=	propelling acceleration ($a_p \triangleq \|\boldsymbol{a}_p\|$)
$a_\oplus$	=	sailcraft characteristic acceleration

---

[*]Research Assistant, Department of Aerospace Engineering, a.quarta@ing.unipi.it. Senior Member AIAA.

[†]Associate Professor, Department of Aerospace Engineering, g.mengali@ing.unipi.it. Senior Member AIAA.

e	$=$	initial orbit eccentricity
$\mathcal{E}$	$=$	mechanical specific energy
F	$=$	maximum propelling thrust at $r = r_\oplus$
H	$=$	Hamiltonian
k_P	$=$	power subsystem mass margin
k_s	$=$	structure mass margin
L	$=$	total tethers length
l	$=$	tether length
m_0	$=$	sailcraft in-flight total mass
m_E	$=$	electric sail mass
m_p	$=$	platform mass
m_P	$=$	power subsystem mass
m_s	$=$	structure mass
m_{th}	$=$	tethers total mass
n	$=$	tethers number
P	$=$	electron gun power
J	$=$	performance index
r	$=$	Sun-sailcraft distance ($r_\oplus \triangleq 1\,\mathrm{AU}$)
t	$=$	time
u	$=$	radial component of velocity
v	$=$	circumferential component of velocity
V	$=$	sailcraft final velocity modulus
V_∞	$=$	hyperbolic excess speed
α	$=$	sail cone angle
α_λ	$=$	primer vector cone angle
δ	$=$	sail clock angle
η	$=$	specific power
θ	$=$	polar angle
λ_i	$=$	adjoint variable (with $i = r,\,\theta,\,u,\,v$)
$\mu_\odot$	$=$	Sun's gravitational parameter
σ_F	$=$	propelling thrust density
$\sigma_{m_{th}}$	$=$	tethers mass density
σ_P	$=$	electron gun power density
τ	$=$	switching parameter
$\mathcal{T}_\odot(r,\,\psi,\,\phi)$	$=$	inertial spherical reference frame
$\mathcal{T}_\odot(r,\,\theta)$	$=$	inertial polar reference frame

$\mathcal{T}_L(x_L,\,y_L,\,z_L)$ =   orbital reference frame
ϕ =   ecliptic latitude
ψ =   ecliptic longitude

Subscripts

0   =   initial
1   =   perihelion
2   =   final
100   =   100 AU
c =   cutoff
on   =   electric sail on
H =   heliopause nose
max   =   maximum
min   =   minimum

Superscripts

$\cdot$ =   time derivative
$-$ =   mean over $\theta_0 \in [0, 2\pi]$

Introduction

The scientific importance of sending a spacecraft to the outer Solar System (SS) boundaries is widely accepted as the primary means to obtain a more comprehensive knowledge of the heliosphere and the nearby interstellar medium. A number of key open questions about those unexplored regions still exist as, for example, the distribution of matter in the outer SS, the chemical evolution of our galaxy, the structure and dynamics of the heliosphere, and the nature and properties of the nearby galactic medium. Currently, only two spacecraft, Voyager 1 and 2, having reached the SS boundaries, are capable of obtaining in situ information.

Voyager 1 crossed the termination shock (where the solar wind speed changes from being supersonic to subsonic) on December 2004, at a distance of 94 AU from the Sun, becoming the first spacecraft to begin exploring the heliosheath, the outermost layer of the heliosphere [1]. Voyager 2 has performed several crossings of the termination shock between 30 August and 1 September 2007. Since then, Voyager 2 has remained in the heliosheath [2]. Although Voyager 1 and 2 are making fundamental discoveries, their instruments were designed to investigate the outer planets and their satellites. Therefore, there are many properties that Voyager's 30-years old instruments are unable to measure. New missions are necessary, with specifically designed instruments, to make comprehensive measurements and deepen human knowledge of the SS boundaries.

Those very long distances from the Sun, on the order of $100 - 200$ AU, take a long time to be reached using conventional (chemical) or advanced (solar and nuclear electric) propulsion technology, even when combined with planetary and solar gravity assists [3]. Therefore, a primary requirement of new missions is the use of exotic propulsion systems. Not surprisingly, a number of recent mission studies towards the heliospheric boundaries and the nearby interstellar space are based on the employment of solar sails [4, 5]. In fact, until now, solar sailing has proven to be the only feasible solution to reach the heliopause nose, at a distance of about 200 AU, with a flight time of 25 years and a final SS escape velocity of approximately 10 AU/year [6, 7].

From a mission analysis point of view, the propensity to choose such an innovative propulsion system for reaching the boundaries of the SS is basically due to two main reasons. One one side it is connected to the characteristic of solar sails to producing thrust without any propellant. This peculiarity allows a solar sail to continuously provide a propelling acceleration for the whole long mission time, on the order of some dozen years. In fact, the time interval in which the sail may produce thrust is indeed theoretically infinite, if one neglects

the degradation effects of the reflective film [8–11] due to the interactions with the solar light [12]. The second reason is that the solar sail can gain a large amount of ΔV in a reasonable amount of time by making a close approach to the Sun [5, 13, 14].

Excluding the minimagnetospheric plasma propulsion (M2P2) [15–18], which requires a certain amount of propellant to create a large magnetic plasma bubble around the spacecraft, the two previous characteristics were, until recently, a prerogative of solar sails alone. Currently an alternative exists, because the electric sail [19] is theoretically capable of fulfilling similar requirements for missions towards the SS boundaries. The electric sail is an innovative propulsion concept that uses the solar wind dynamic pressure for generating a thrust without the need for reaction mass [19–21]. The spacecraft is spun around a symmetry axis and uses the centrifugal force to deploy and stretch out a number of thin, long, conducting tethers [22]. The latter are held at high positive potential by an electron gun, whose electron beam is shot roughly along the spin axis. The resulting static electric field of the tethers perturbs the trajectories of the incident solar wind protons, thus producing a momentum transfer from the solar wind plasma stream to the tethers.

The electric sail thrust concept has been used to calculate successful and efficient mission trajectories in the SS for realistic payloads [22–24]. However, a detailed study regarding the feasibility of reaching the SS boundaries has not yet been performed. The aim of this paper is to provide alternative results and preliminary mission studies using an electric sail as a primary propulsion system. In particular, a key point is to investigate whether an electric sail is suitable for reaching either the heliosheath or the heliopause nose in a reasonable flight time and with a launch mass comparable to that required by a solar sail.

The paper is organized as follows. First, the electric sail minimum time performance, necessary to reach a given hyperbolic excess speed with respect to the Sun system, is studied in a two-dimensional framework. This analysis provides preliminary information on the effect

of a close approach to the Sun (to increase the sailcraft available thrust) on an escape mission from the SS. Then, the minimum flight times required to reach a prescribed distance from the Sun is calculated using a planar model. Such information are employed as a starting point for a three dimensional analysis of the problem, which takes into account the actual position of the heliopause nose. Finally, the obtained results are used, with the aid of a suitable mass distribution model, to get an estimate of the sailcraft mass characteristics.

Problem Description

Consider an electric sail placed on a heliocentric elliptic orbit with given values of semi-major axis a and eccentricity e, and let r_0 be the sailcraft distance from the Sun at the initial time t_0. The electric sail trajectory for $t > t_0$ is studied with the aid of a helio-centric polar reference frame $\mathcal{T}_\odot(r, \theta)$, where the polar angle θ is measured anticlockwise from a fixed direction. The generic sailcraft trajectory, illustrated in Fig. 1, may include a close approach to the Sun for increasing the sailcraft propelling acceleration. However, the Sun-sailcraft distance cannot decrease below a minimum admissible value $r_{\min}$ imposed by thermal constraints.

In a first phase of our study we assume a two-dimensional problem in which the orbital plane coincides with the ecliptic plane. This allows one to obtain a first estimate of the electric sail minimum time performance for a number of mission scenarios. The obtained results will be then refined with a three dimensional analysis of specific missions in the second part of the paper. In a two-dimensional problem the sailcraft velocity may be decomposed into a radial u and a circumferential v velocity components. Let t_1 be the time instant in which the sailcraft reaches the minimum distance from the Sun, and t_2 the time of mission end. The problem addressed here is to minimize the time t_2 necessary to transfer the spacecraft from an initial given state $[r(t_0), \theta(t_0), u(t_0), v(t_0)]$ to a final prescribed state $[r(t_2), \theta(t_2), u(t_2), v(t_2)]$. This
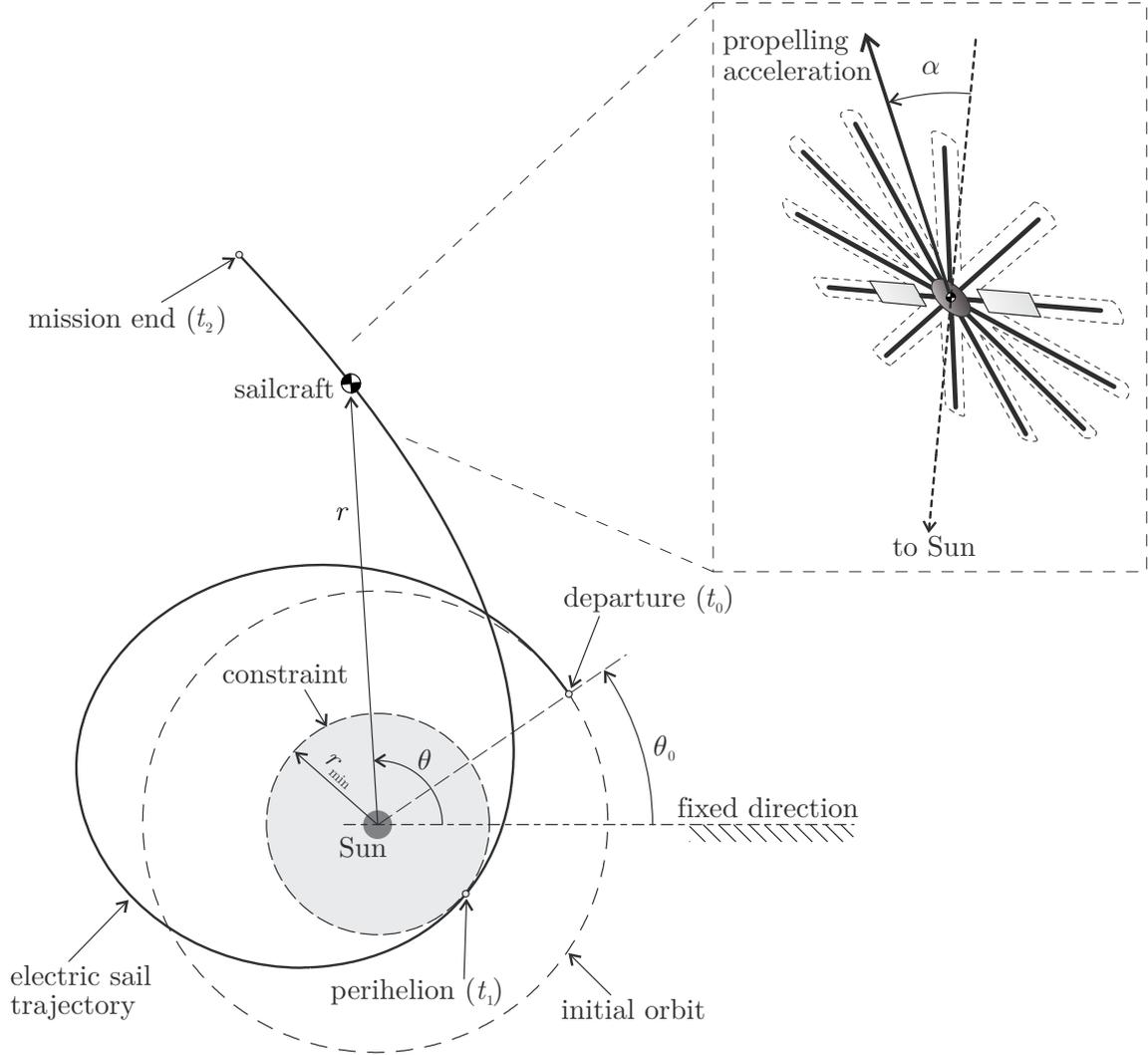
Figure 1: **Polar reference frame and typical electric sail two-dimensional trajectory.**

amounts to maximizing the scalar performance index

$$J = -t_2 \tag{1}$$

The electric sail trajectory may be tuned through two independent control variables, τ and α. The switching parameter $\tau = (0, 1)$ models the thruster on/off condition, and is introduced to account for coasting arcs in the spacecraft trajectory. The second control variable, that is, the sail cone angle α, coincides with the angle between the Sun-sailcraft line and the thrust

direction, see Fig. 1. The value of α may be adjusted in the range $[-\alpha_{\mathrm{max}}, \alpha_{\mathrm{max}}]$ by suitably orienting the plane containing the sail tethers as described in Ref. [22].

The electric sail propelling acceleration modulus depends on the sailcraft distance from the Sun as [22, 25]

$$a_p = a_\oplus \left(\frac{r_\oplus}{r}\right)^{7/6} \tag{2}$$

where $a_\oplus$, referred to as sail characteristic acceleration, is the maximum propelling acceleration at $r = r_\oplus \triangleq 1\,\mathrm{AU}$. Accordingly, $a_\oplus$ is the parameter commonly used to quantify the electric sail performance. The problem of maximizing the performance index J may be addressed with an indirect approach, and its solution is described elsewhere [22]. For the sake of completeness, the appendix summarizes the four first order differential equations necessary to describe the electric sail motion, Eqs. (17–20), and the corresponding four Euler-Lagrange equations, Eqs. (22–25). A total of eight suitable boundary conditions are therefore required to complete the mathematical problem, whereas a further scalar relationship is necessary to find the final time t_2.

Assume that the polar angle θ is measured from the apse line of the initial orbit. Then $\theta_0 \triangleq \theta(t_0)$ is the electric sail true anomaly at departure. The four initial boundary conditions are

$$\theta(t_0) = \theta_0 \quad , \quad r(t_0) = \frac{a\,(1 - e^2)}{1 + e\,\cos\theta_0}$$

$$u(t_0) = \frac{e\,\sin\theta_0}{\sqrt{a\,(1 - e^2)/\mu_\odot}} \quad , \quad v(t_0) = \frac{1 + e\,\cos\theta_0}{\sqrt{a\,(1 - e^2)/\mu_\odot}} \tag{3}$$

The remaining four boundary conditions at the final time t_2 depend on the particular mission typology and are discussed in the next section.

Mission Scenarios

Electric sail trajectories towards the SS boundaries are now investigated with different requirements and, correspondingly, different mission typologies.

Achievement of a Given Hyperbolic Excess Speed

In this first mission scenario, the sailcraft is required to reach a given hyperbolic excess speed $V_\infty \geq 0$ with respect to the Sun system in the least possible amount of time. The rationale for such a strategy is that V_∞ essentially coincides with the sailcraft cruise speed (that is, a uniform rectilinear motion [26]) in a hyperbolic trajectory towards the interstellar deep space. An early achievement of a substantial value of hyperbolic excess speed allows the spacecraft to jettison the electric sail. This simplifies the succeeding mission phases, thereby avoiding potential interferences with the payload instruments, and reduces the likelihood of a mission failure. Such a strategy has been proposed for similar deep space missions based on solar sails [4, 27].

From a mathematical viewpoint, the problem amounts to prescribing the sailcraft mechanical energy $\mathcal{E}$ at the final instant t_2, that is

$$\mathcal{E}(t_2) \triangleq \frac{u(t_2)^2 + v(t_2)^2}{2} - \frac{\mu_\odot}{r(t_2)} = \frac{V_\infty^2}{2} \tag{4}$$

The three remaining boundary conditions necessary to obtain a stationary value of J involve the adjoint variables, viz [28]

$$\lambda_\theta(t_2) = 0 \quad , \quad \lambda_u(t_2) = \frac{\lambda_r(t_2)\, u(t_2)\, r(t_2)^2}{\mu_\odot} \quad , \quad \lambda_v(t_2) = \frac{\lambda_r(t_2)\, v(t_2)\, r(t_2)^2}{\mu_\odot} \tag{5}$$

The optimization problem is constituted by a two-point boundary value problem (2PBVP) whose differential equations are shown in the appendix, and whose eight boundary conditions

are given by Eqs. (3), (4) and (5). The final time t_2 is obtained by enforcing the transversality condition

$$H(t_2) = 1 \tag{6}$$

Note that the mission typology described in this section includes, as a particular case, the escape trajectories from the SS. In fact, the latter are obtained by setting the hyperbolic excess velocity equal to zero in Eq. (4), or, equivalently, $\mathcal{E}(t_2) = 0$.

Achievement of a Given Solar Distance

As a second mission scenario, consider the minimum time trajectories to reach a given distance $r_2 > r(t_0)$ from the Sun. These missions include both rapid flyby trajectories towards the outer planets and transfers towards the SS boundaries or the heliosheath [4, 27, 29]. The main difference with respect to the problem discussed in the previous section is that now the parameter to minimize is the mission time necessary to reach r_2 irrespective of the value of V_∞. As a result, because the final hyperbolic excess speed is not explicitly used in the optimization process, in principle it is possible that the spacecraft cruise velocity at a distance r_2 be insufficient to continue the mission towards the deep space [29].

Using the final distance as the unique constraint on the probe trajectory (that is, both the spacecraft final angular position and its velocity components are left free), the following four boundary conditions are obtained at $t = t_2$:

$$r(t_2) = r_2 \quad , \quad \lambda_\theta(t_2) \equiv \lambda_u(t_2) \equiv \lambda_v(t_2) = 0 \tag{7}$$

As in the previous case, the flight time t_2 is found through Eq. (6), which, associated to Eqs. (3) and (7), completes the 2PBVP.

Constraints on Minimum Perihelion Distance

So far, no explicit constraint has been imposed on the minimum perihelion distance of the spacecraft trajectory. However, in both of the two preceding mission scenarios it is possible that, in an initial phase, the sailcraft goes towards the Sun to exploit the increased available thrust resulting from the growing solar wind electron density and temperature [19, 20, 22]. Such a behavior, which will be referred to as solar wind assist (SWA), is similar (albeit based on a different physical mechanism) to the more familiar solar photonic assist concept [14, 30, 31], frequently used in solar sail based missions [4, 27, 29]. When a mission includes a SWA maneuver, it is necessary to guarantee that the sailcraft heliocentric distance does not fall below some $r_{\min} > 0$, that is, a minimum admissible value based on thermal and mechanical constraints involving the electric sail tethers. Preliminary estimates suggest assuming $r_{\min} = 0.5\,\mathrm{AU}$ when aluminium tethers are used, while copper tethers are expected to guarantee a further reduction in the minimum distance up to $r_{\min} = 0.33\,\mathrm{AU}$ (Janhunen P., private communication, 2009).

From a mathematical point of view, the requirement on minimum perihelion distance can be taken into account with the addition of an inequality path constraint on the state variable r in the form [28]:

$$r(t_1) \geq r_{\min} \qquad \text{for} \qquad t_1 \in [t_0, t_2) \tag{8}$$

where t_1 is the time instant at which the minimum Sun-sailcraft distance is reached. In practice, the optimal problem can be solved through a two step procedure. Firstly, a solution is found without imposing any path constraint. Let $r^\star$ be the minimum resulting distance from the Sun. If $r^\star \geq r_{\min}$, the corresponding trajectory is truly optimal and no further calculation is necessary. If, instead, $r^\star < r_{\min}$ (thus implying that the constraint (8) would be violated), a second step is required. More precisely, a switching structure is assumed a

priori [28], the constraint (8) (taken with the equality sign) is set active at $t = t_1$, and the sailcraft trajectory is divided into two arcs, corresponding to the approaching and departure phases, respectively. Invoking the transversality condition [28], the following two scalar relationships are found at the (unknown) time instant t_1

$$r(t_1) = r_{\min} \quad , \quad u(t_1) = 0 \tag{9}$$

It may be shown that λ_r is the only adjoint variable discontinuous at t_1. In other terms, a three point boundary value problem (3PBVP) is now involved, in which both the time instant t_1 and the discontinuity (that is, the jump) in λ_r are found by imposing the two intermediate conditions (9). Note that the initial conditions (3), the final conditions (5) [or (7)] and the transversality condition (6), remain all unchanged.

Numerical Approach

The 2PBVP (or 3PBVP) associated to the variational problem has been solved through a hybrid numerical technique that combines genetic algorithms (to obtain an estimate of the initial adjoint variables), with gradient-based and direct methods to refine the solution [32, 33]. A set of canonical units [34] have been used in the integration of the differential equations to reduce their numerical sensitivity. The differential equations were integrated in double precision using a variable order Adams-Bashforth-Moulton solver [35, 36] with absolute and relative errors of 10^{-12}. The final boundary constraints were set to $100\,\mathrm{km}$ for the position error and $0.05\,\mathrm{m/s}$ for the velocity error. These tolerance limits are sufficient for a preliminary mission analysis study.

Solar System Escape Trajectories

Consider first the problem of generating trajectories that allow an electric sail to escape from the SS using an Earth-escape parabolic trajectory, that is, with zero hyperbolic excess energy with respect to the planet (launch $C_3 \equiv 0\,\mathrm{km^2/s^2}$). This amounts to selecting $V_\infty = 0$ (or $\mathcal{E}(t_2) = 0$) in Eq. (4). The sensitivity of the minimum flight time t_2 to the sail performance has been studied in a parametric form, by varying the sailcraft characteristic acceleration $a_\oplus$ in the range $[0.5, 2]\,\mathrm{mm/s^2}$. The upper limit corresponds to an estimated maximum value of the propelling acceleration at $r = r_\oplus$ that will be probably available in a near future. Two cases have been studied, corresponding to either a circular or an elliptical parking orbit. In both cases the maximum allowed cone angle is $\alpha_{\mathrm{max}} = 35\,\mathrm{deg}$, while the minimum perihelion distance is set to $r_{\mathrm{min}} = 0.5\,\mathrm{AU}$.

Escape from a circular orbit

In this first case the starting orbit is circular with a radius equal to $1\,\mathrm{AU}$. Accordingly, t_2 is independent of the sailcraft initial position (that is, of the launch date). This amounts to setting $\theta_0 = 0$, $e = 0$, and $a = 1\,\mathrm{AU}$ in Eqs. (3). The mission times obtained from simulations are shown in Fig. 2 as a function of the characteristic acceleration.

The escape time is tolerable, being less than $4.6\,\mathrm{years}$, even for moderate values of the characteristic acceleration. Note that as long as $a_\oplus$ is less than $0.55\,\mathrm{mm/s^2}$, the optimal escape condition is reached without activating the constraint on r_{min}. When the value of the characteristic acceleration ranges in the interval $[0.54, 1.16]\,\mathrm{mm/s^2}$, the spacecraft trajectory tends to approach the Sun closer to exploit the thrust rise associated to the SWA. Accordingly, the constraint on the minimum admissible perihelion distance is activated. However, there exists a critical value of characteristic acceleration (equal to about $1.16\,\mathrm{mm/s^2}$) over which the escape condition is more quickly obtained using a direct transfer (DT), that is, using a trajectory that increases, at any time, the instantaneous sailcraft distance from
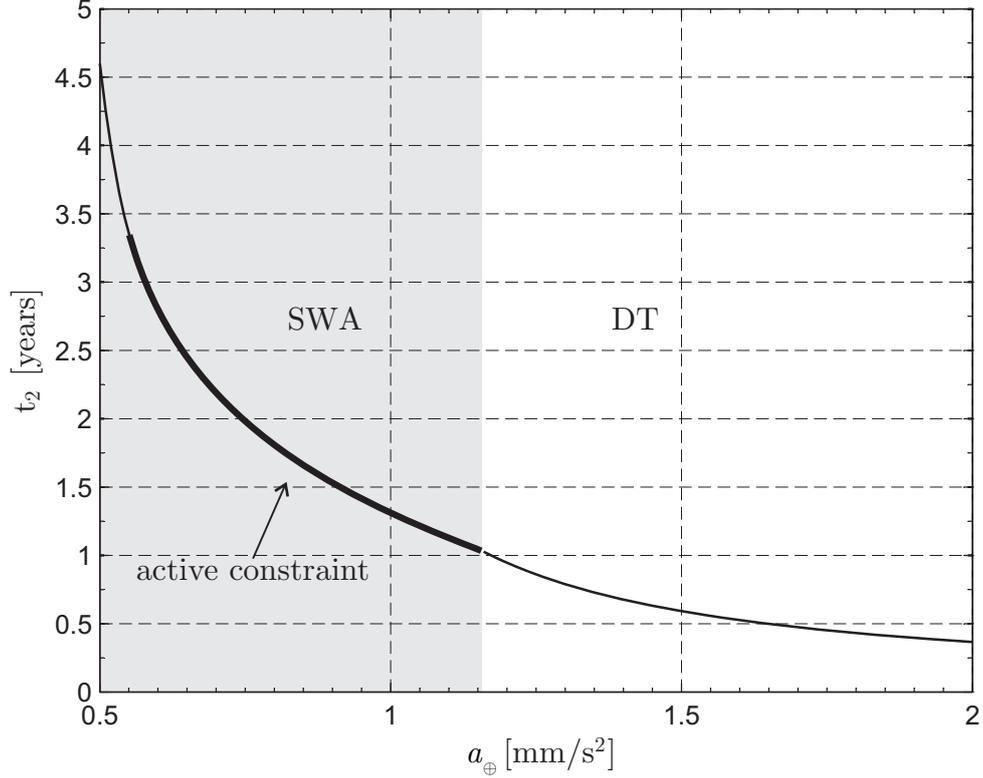
Figure 2: Minimum escape times from Earth circular orbit ($r_{\min} = 0.5\,\mathrm{AU}$).

the Sun. The spacecraft behavior is better understood with the aid of Fig. 3, which illustrates the sailcraft trajectory for three different values of characteristic acceleration. In particular, the three typologies correspond to a SWA trajectory with inactive constraint ($a_{\oplus} = 0.5\,\mathrm{mm/s^2}$), a SWA trajectory with active constraint ($a_{\oplus} = 1\,\mathrm{mm/s^2}$) and a DT trajectory ($a_{\oplus} = 1.5\,\mathrm{mm/s^2}$). Moreover, it may be shown by simulation that in a SWA strategy the minimum perihelion distance tends to continuously reduce as $a_{\oplus}$ is increased, see Fig. 8. A similar behavior was pointed out by Sauer [4] in his analysis of escape missions with solar sails.

Returning now to the three cases of Fig. 3, it is interesting to study the behavior of the specific mechanical energy $\mathcal{E}$ as a function of time, see Fig. 4. During a SWA trajectory there is a time interval characterized by $\dot{\mathcal{E}} < 0$, (a phase in which the sail thrust is used for approaching the Sun) and a coasting phase ($\mathcal{E} = \mathrm{constant}$). On the contrary, in a DT
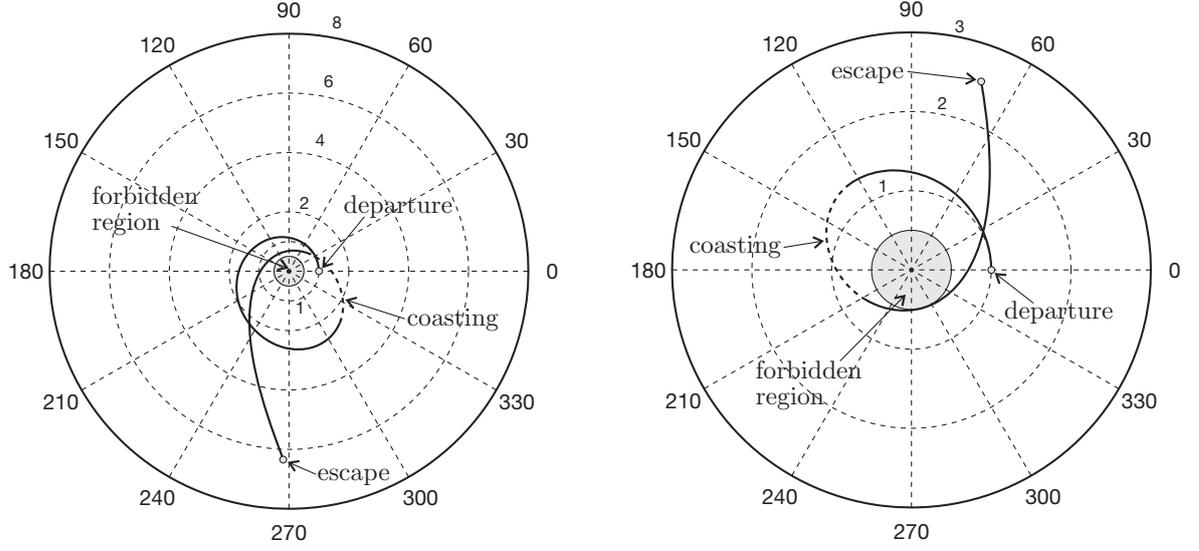
a) SWA with inactive constraint $(a_\oplus = 0.5\,\mathrm{mm/s^2},\ t_2 \simeq 4.6\,\mathrm{years})$.

b) SWA with active constraint $(a_\oplus = 1\,\mathrm{mm/s^2},\ t_2 \simeq 1.31\,\mathrm{years})$.
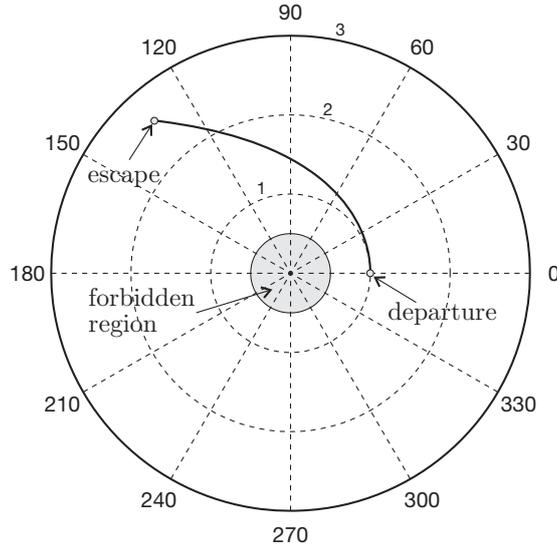
c) DT $(a_\oplus = 1.5\,\mathrm{mm/s^2},\ t_2 \simeq 0.59\,\mathrm{years})$.

Figure 3: **Escape trajectories from an Earth circular orbit $(r_{\min} = 0.5\,\mathrm{AU})$.**

trajectory the function $\dot{\mathcal{E}}$ is always positive and, therefore, $\tau \equiv 1$. In other terms the DT may be thought of as the globally optimal counterpart of a locally optimal strategy [37–41], where the controls are chosen to maximize, at any time, the instantaneous variation of the mechanical energy $\dot{\mathcal{E}}$. The length of a coasting phase in a SWA trajectory is strongly
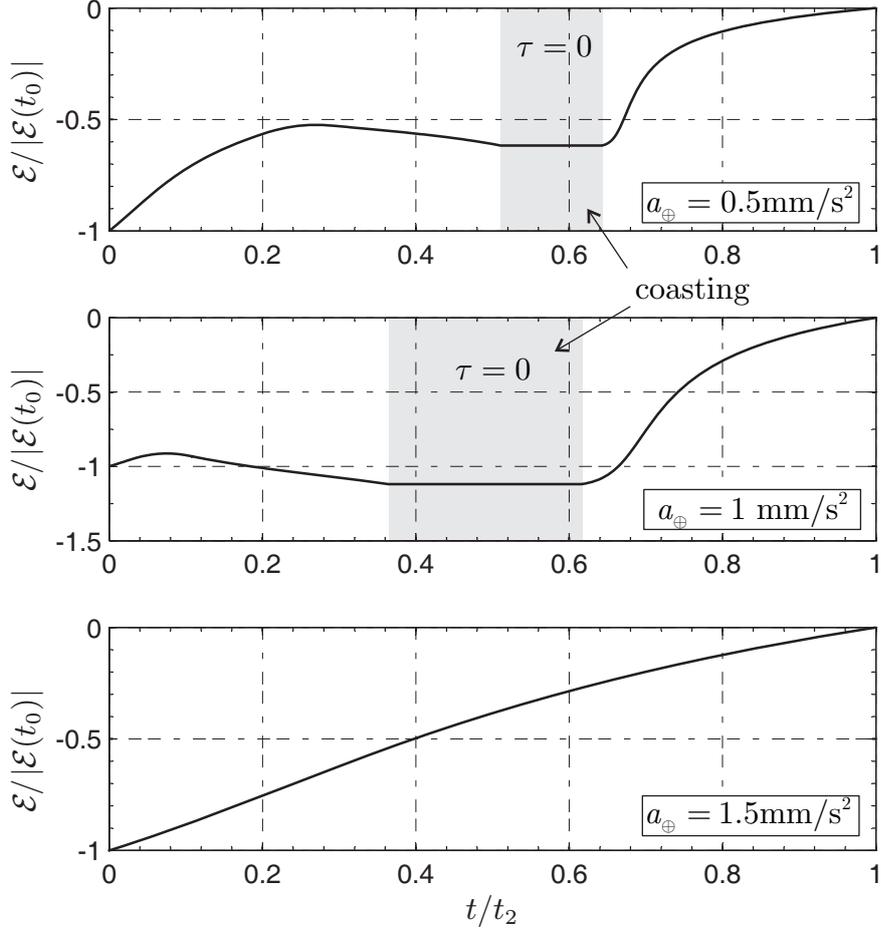
Figure 4: Mechanical energy vs. time for optimal escape trajectories ($r_{\min} = 0.5\,\mathrm{mm/s^2}$).

dependent on the value of the characteristic acceleration. Figure 5 compares the sail cone angle $\alpha(t)$ for the three cases with $a_\oplus = (0.5,\ 1,\ 1.5\,\mathrm{mm/s^2})$. While in a DT α is constant and equal to $\alpha_{\max} = 35\,\mathrm{deg}$ during the whole mission, in a SWA trajectory the cone angle experiences a sign variation during the perihelion approaching phase ($t \in [t_0,\ t_1]$). In terms of escape times, SWA and DT are equivalent strategies when $a_\oplus = 1.16\,\mathrm{mm/s^2}$ (in both cases $t_2 \simeq 1.03\,\mathrm{years}$). However, the corresponding escape distances $r(t_2)$ are much different, as illustrated in Fig. 6. The discontinuity in the crossing between the two strategies is better highlighted in Fig. 7, which shows the escape distance as a function of $a_\oplus$. The sensitivity of the escape time with respect to the value of $r_{\min}$ is shown Fig. 8. The flight times have
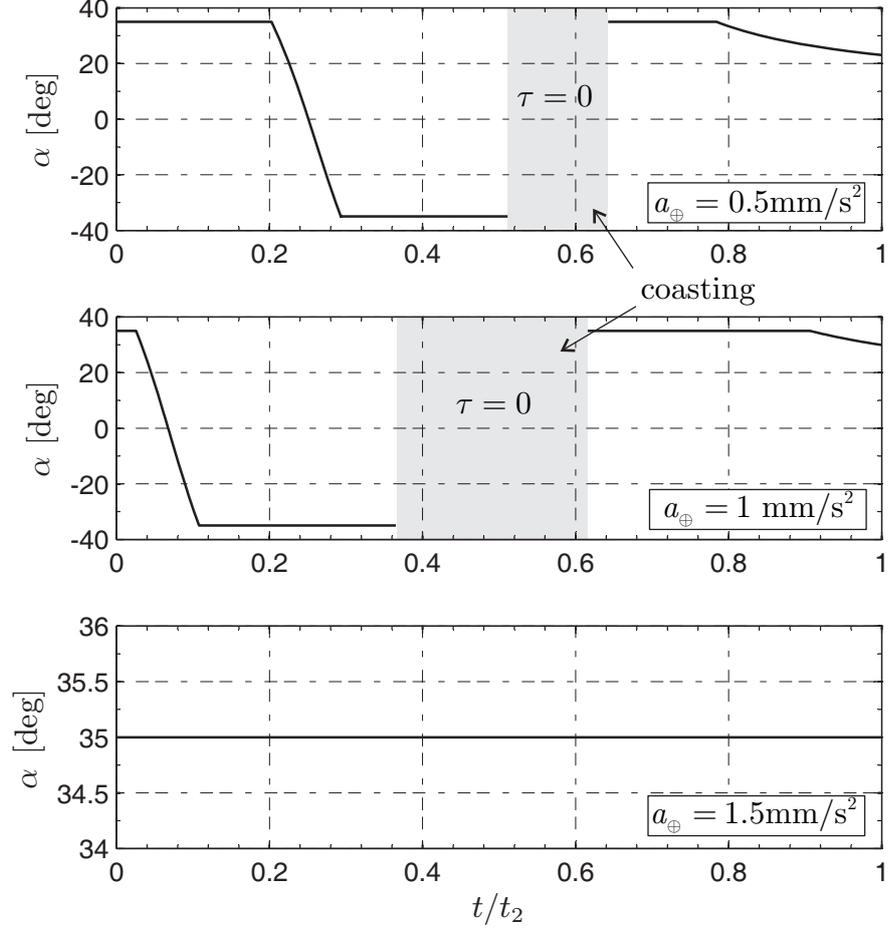
Figure 5: Sail cone angle for minimum-time escape trajectories ($r_{\min} = 0.5\,\text{mm/s}^2$).

been normalized by the escape times corresponding to $r_{\min} = 0.5\,\text{AU}$, and taken from Fig. 2. The analysis is confined to the range $a_\oplus \in [0.55,\ 1]\,\text{mm/s}^2$, within which from our previous discussion $r(t_1) = 0.5\,\text{AU}$. Figure 8 shows that the performance improvements obtained by decreasing $r_{\min}$ are moderate. For example, assuming $r_{\min} = 0.33\,\text{AU}$ (copper tethers), the reduction of escape time with respect to $r_{\min} = 0.5\,\text{AU}$ is less than 8%.

Escape from an elliptic orbit

In this case the initial orbit coincides with the real heliocentric orbit of Earth, that is, $a = 1\,\text{AU}$ and $e = 0.01671123$. Because the polar symmetry is lost, the mission performance must be studied by varying the initial true anomaly in the range $\theta_0 \in [0,\ 2\pi]$. It may be

a) SWA.   **b)** DT.
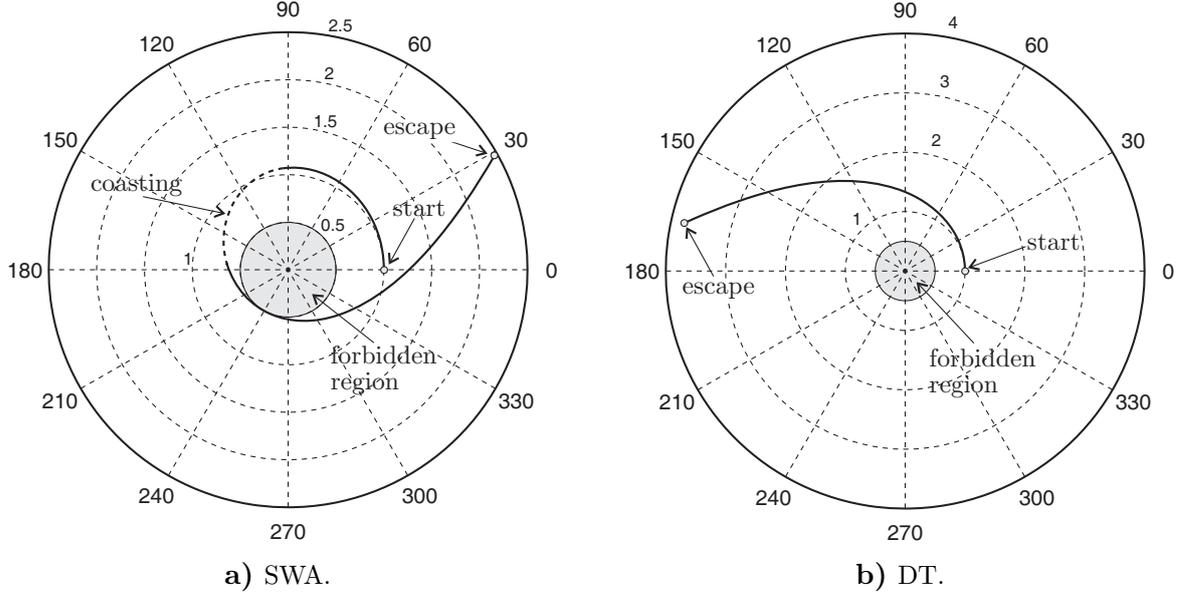
Figure 6: Escape trajectory from Earth circular orbit for $a_\oplus = 1.16\,\mathrm{mm/s^2}$ ($t_2 \simeq 1.03\,\mathrm{years}$).
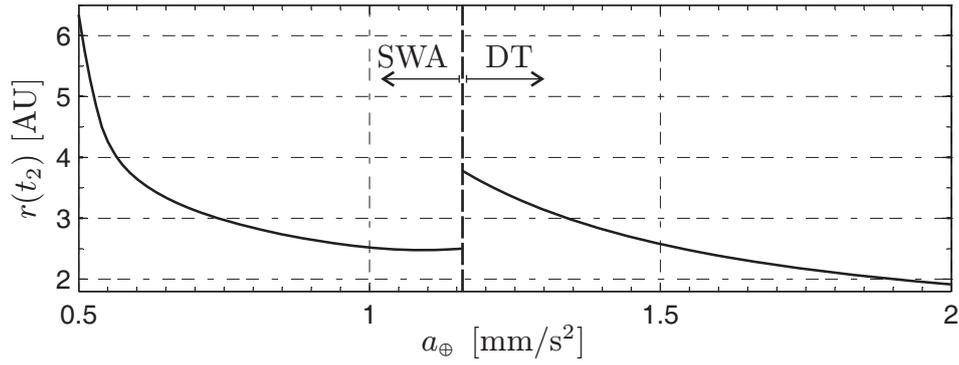
Figure 7: Final distance for escape trajectories from Earth circular orbit as a function of $a_\oplus$ ($r_{\min} = 0.5\,\mathrm{AU}$).

verified that the transition between SWA and DT strategies is essentially independent of θ_0 and is obtained when $a_\oplus \simeq 1.2\,\mathrm{mm/s^2}$. With reference to Fig. 9, the escape time t_2 is made dimensionless with its mean value $\bar{t}_2$ (calculated over θ_0) and the results have been separated according to the best escape strategy (either SWA or DT). The initial orbit eccentricity has a negligible effect on t_2 because the variation of $t_2/\bar{t}_2$ is always less than 5% when $a_\oplus$ ranges in the interval $[0.5,\,2]\,\mathrm{mm/s^2}$. The optimal launch position in terms of θ_0 and the corresponding escape times have been summarized in Table 1. Note that the last table column shows the
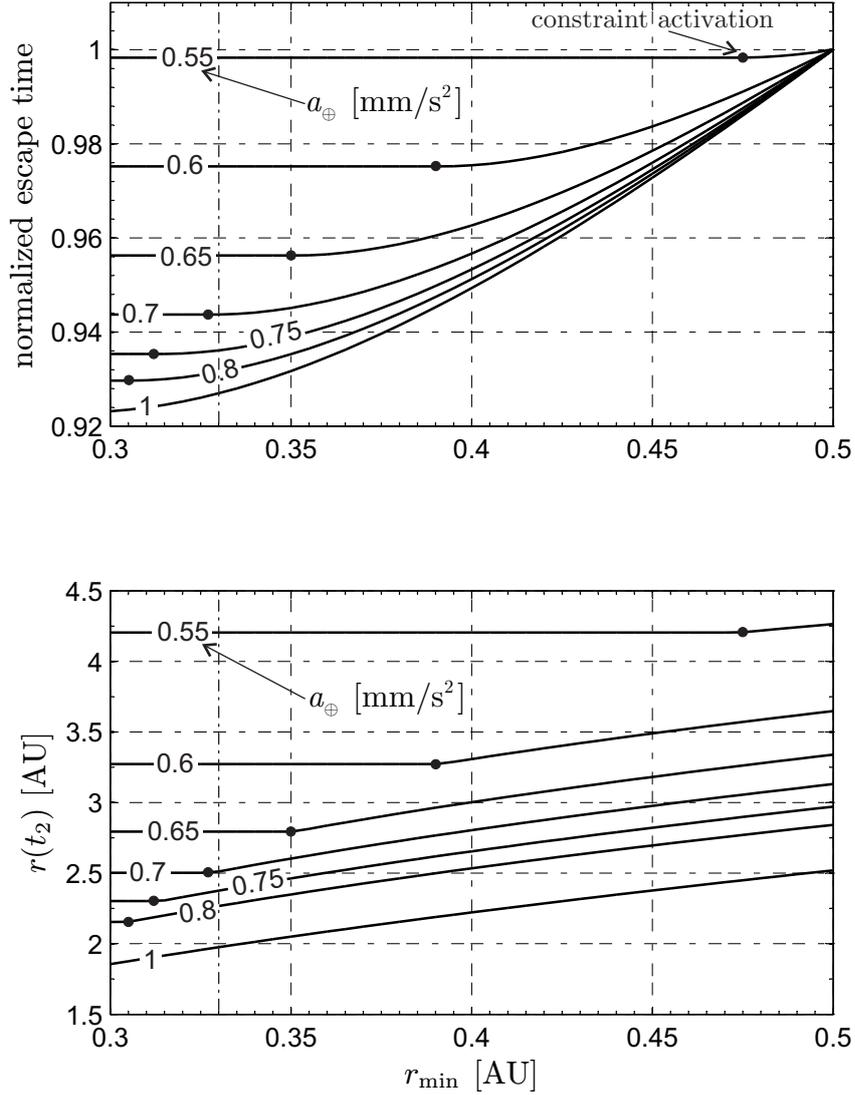
Figure 8: **Escape time from Earth circular orbit and final distance as a function of** $a_\oplus$ **and** $r_{\min}$.

number of electric sail revolutions around the Sun prior to the escape condition attainment, while the second column summarizes the minimum escape times from a circular Earth orbit (see Fig. 2).

Two-Dimensional Trajectories Towards the Outer Solar System

In the previous section we have calculated the minimum time necessary to insert the electric sail into a parabolic orbit. Once the escape condition is met, the propelling system
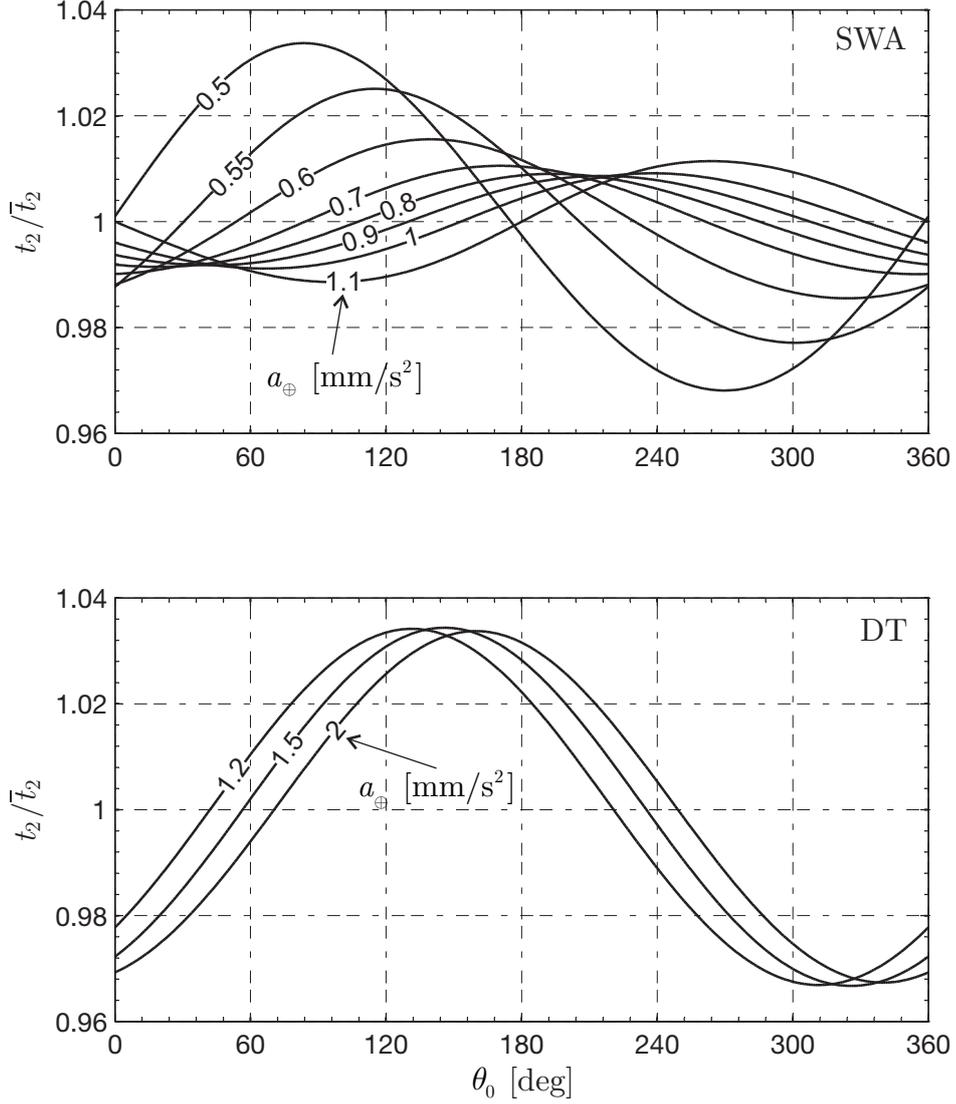
Figure 9: Escape times from Earth elliptic orbit as a function of $a_\oplus$ and θ_0.

may be jettisoned in such a way that the payload alone can continue its travel towards the deep space with a flight by inertia. Suppose now that the mission aim is to reach a given solar distance $r_2 \in [5, 100\,\mathrm{AU}]$ in the least amount of time. To avoid very long mission lengths, greater than 20 years when $r_2 = 100\,\mathrm{AU}$, we will consider electric sails with medium-high performance characterized by $a_\oplus \in [1, 2]\,\mathrm{mm/s^2}$. A preliminary analysis of this problem confirms that the Earth's orbital eccentricity has a negligible effect on the mission performance. Therefore, the initial parking orbit is assumed to be circular with a radius

$a_\oplus$ [mm/s^2]	t_2 ($e=0$) [years]	Optimal Conditions						
		θ_0 [deg]	t_1 [years]	$r(t_1)$ [AU]	$r(t_2)$ [AU]	$\theta(t_2)$ [deg]	t_2 [years]	revs.
0.5	4.599	270	2.993	0.6379	6.1499	174.38	4.449	1
0.6	2.802	324	2.094	0.5	3.6179	146.71	2.762	1
0.7	2.193	355	1.620	0.5	3.1205	136.55	2.172	1
0.8	1.811	19	1.305	0.5	2.8379	131.91	1.795	1
0.9	1.532	42	1.067	0.5	2.6476	130.8	1.519	1
1	1.314	67	0.8717	0.5	2.5281	132.89	1.302	1
1.1	1.131	96	0.6851	0.5	2.5064	136.68	1.118	1
1.2	0.946	311	0	0.9884	3.4933	113.21	0.9146	0
1.3	0.789	317	0	0.9873	3.0742	107.31	0.7629	0
1.4	0.676	322	0	0.9864	2.7623	102.92	0.6537	0
1.5	0.592	326	0	0.9858	2.5233	97.46	0.5719	0

Table 1: **Optimal conditions for escape from Earth elliptic orbit ($r_{\min} = 0.5\,\text{AU}$).**

equal to 1 AU. The solutions of the optimal problem with boundary conditions given in Eq. (7) and a minimum perihelion distance $r_{\min} = 0.5\,\text{AU}$ are summarized in Fig. 10.

The DT strategy is superior to the SWA in the grey region highlighted in Fig. 10. This region is confined to rather small values of r_2 when compared to the characteristic dimensions of the SS and to the heliosheath distance (roughly 100 AU). For example, assuming the maximum admissible value of characteristic acceleration, that is, $a_\oplus = 2\,\text{mm/s}^2$, a DT is superior to a SWA transfer provided that $r_2 < 13\,\text{AU}$. In particular, Fig. 10 shows that for medium-high performance electric sails (with $a_\oplus \in [1,\,2]\,\text{mm/s}^2$) a rapid flyby trajectory towards Jupiter (or to the asteroid belt) favors a DT. When rapid flybys towards Saturn are concerned, a SWA strategy is preferable for electric sails with characteristic accelerations less than $1.1\,\text{mm/s}^2$. Finally, missions towards the outer SS require a SWA strategy unless very high performance electric sails are considered (that is, $a_\oplus > 4\,\text{mm/s}^2$).

The simulations show that in all of the analyzed cases the specific mechanical energy
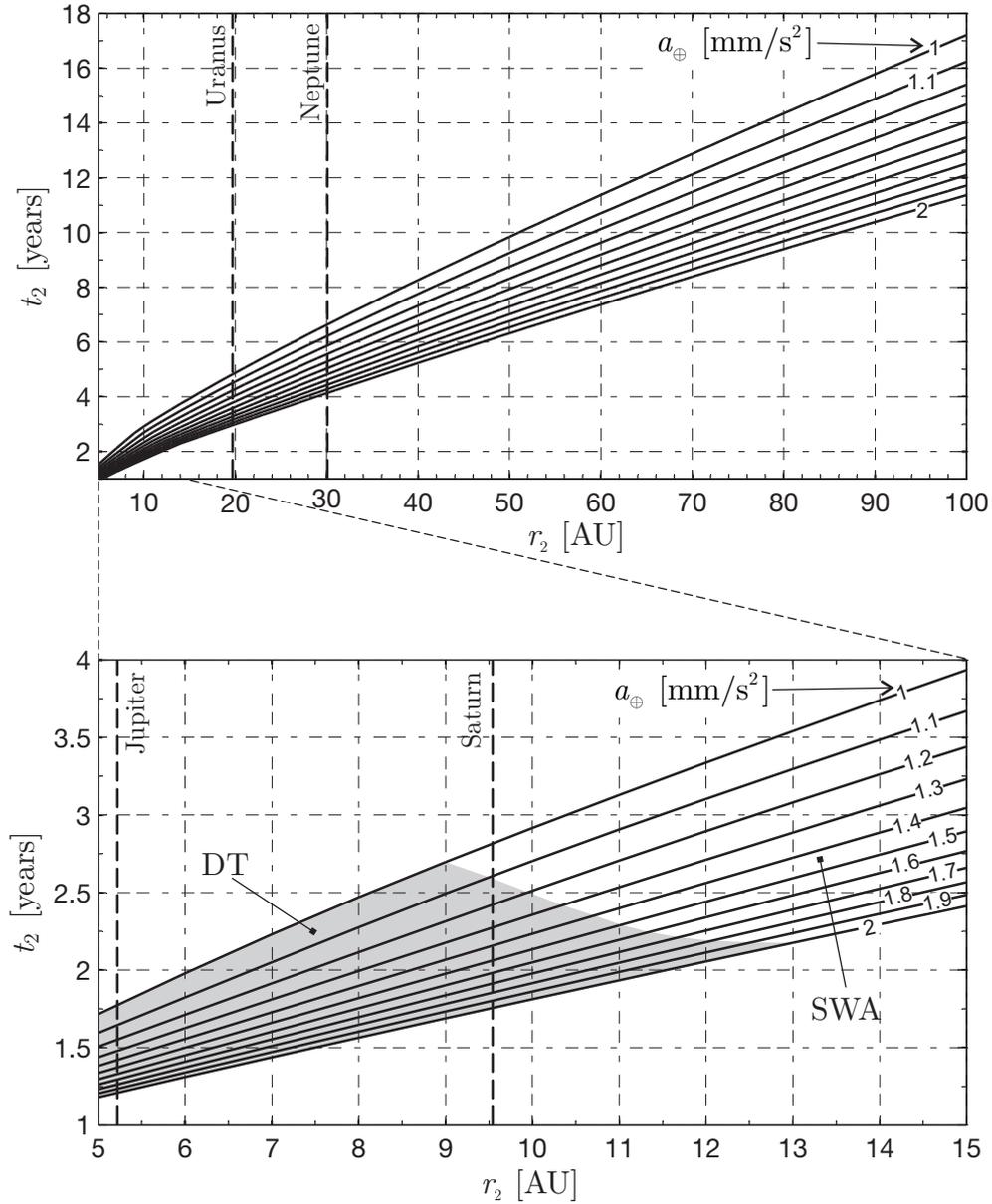
Figure 10: **Minimum flight time t_2 vs. final solar distance r_2 ($r_{\min} = 0.5\,\text{AU}$).**

at r_2 is positive. This means that the sailcraft at the end of its nominal trajectory is on a hyperbolic orbit that eventually leaves the SS. This point is highlighted in Fig. 11 that also shows the value of V_∞ at the final time t_2. Recall, however, that the hyperbolic excess speed shown in Fig. 11 is not the maximum attainable value at $r = r_2$, rather it is the value that the sailcraft obtains at the end of the minimum time trajectory necessary to reach the
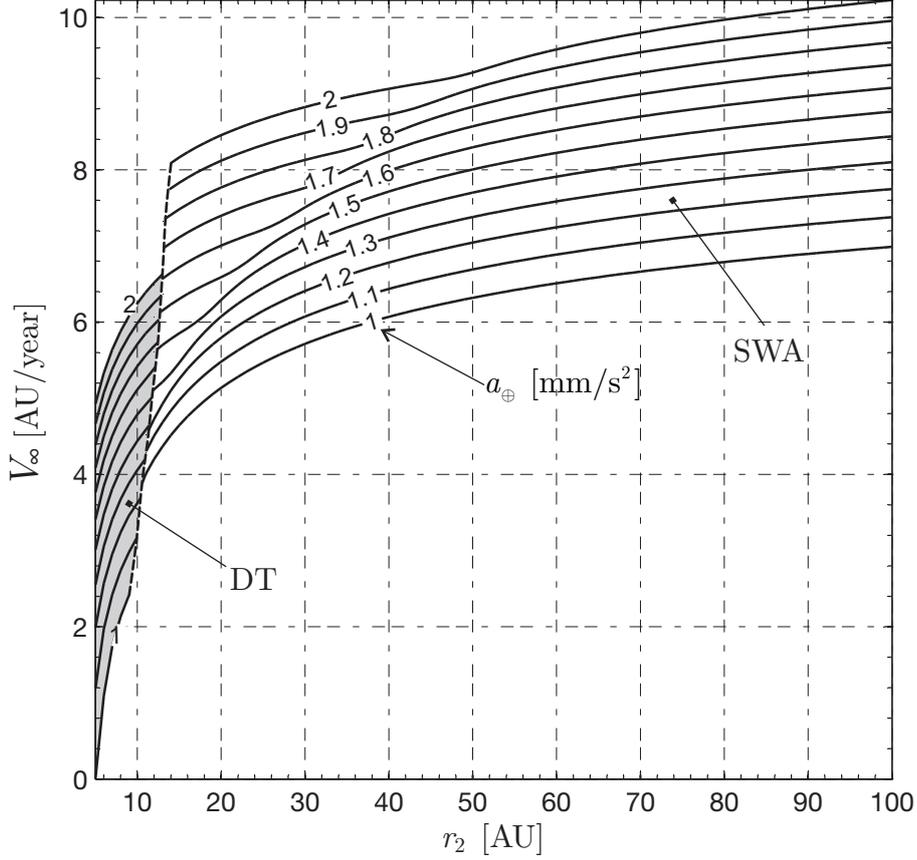
Figure 11: **Hyperbolic excess speed V_∞ as a function of the final solar distance r_2 ($r_{\min} = 0.5\,\text{AU}$).**

desired distance r_2. Note that V_∞ takes high values especially when substantial characteristic accelerations are used. For example, assuming $a_\oplus = 2\,\text{mm/s}^2$, one has $V_\infty \simeq 10\,\text{AU/year}$ at the end of a mission towards the heliosheath ($r_2 \simeq 100\,\text{AU}$). This hyperbolic excess speed is sufficiently high to allow the sailcraft to extend the original mission and continue its travel with a cruise speed roughly coincident with V_∞. To make a comparison with current missions, Voyager 1 is escaping from the SS at a speed of about $3.6\,\text{AU/year}$, while Voyager 2 is escaping at a speed of $3.3\,\text{AU/year}$[1]. Figure 11 shows a discontinuity in the contour line caused by the strategy variation. Note however that this discontinuity is missing in Fig. 10 because the transition between DT and SWA is here controlled by the total mission time

---

[1]Data retrieved from http://voyager.jpl.nasa.gov/mission/interstellar.html [cited 22 April 2009]

and not by the value of V_∞.

The possibility of a mission extension is a particularly important feature for trajectories towards the outer SS space, in which a certain distance must be obtained in a given time and with a prescribed value of hyperbolic excess speed [27]. From this point of view the simulations have shown that the perihelion constraint (in the range $r_{\min} \in [0.3, 0.5]\,\mathrm{AU}$) does not significantly affect the mission performance. This is clear from Fig. 12 in which the flight time t_2 and the hyperbolic excess speed V_∞ are shown as a function of the characteristic acceleration and $r_{\min}$ for minimum time missions towards heliosheath ($r_2 = 100\,\mathrm{AU}$).
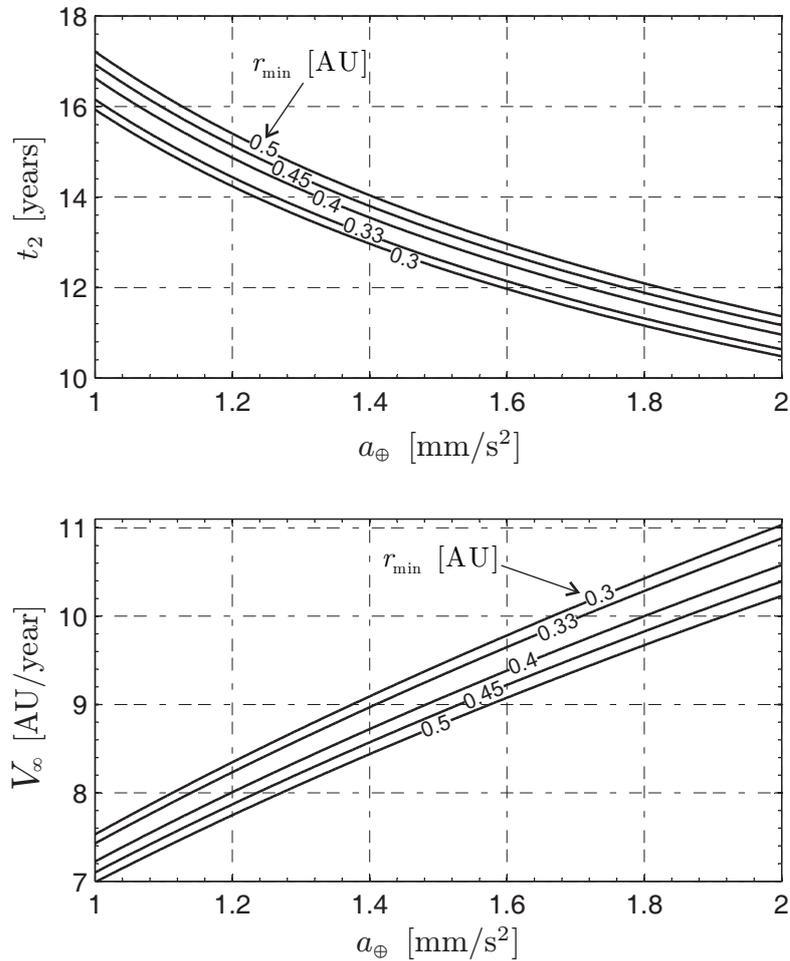
Figure 12: Optimal performance for missions toward the heliosheath ($r_2 = 100\,\mathrm{AU}$).

In particular, assuming $r_{\min} = 0.5\,\mathrm{AU}$, the flight time can be approximated with an error

less than 10 days through the following simplified relationship

$$t_2 \approx \frac{17.18}{a_{\oplus}^{0.6}} \tag{10}$$

in which t_2 is expressed in years, and $a_{\oplus}$ in millimeters per square second. Equation (10) gives a semi-analytic, first order relationship between the time necessary to reach the heliosheath and the electric sail performance in terms of characteristic acceleration. Such a relationship will be the starting point for a second order analysis, discussed in the next section, which takes into account the actual three-dimensionality of the problem at hand.

Figure 12, or Eq. (10) if $r_{\min} = 0.5\,\mathrm{AU}$ is assumed, shows that the heliosheath may be reached in about 15 years with a medium-performance electric sail, having a characteristic acceleration of $1.15 - 1.25\,\mathrm{mm/s^2}$. As a comparative example, Voyager 1 has reached a solar distance of 100 AU in 2006, that is, 29 years after its departure.

In analogy to the escape trajectories from the SS, missions towards the heliosheath are characterized by the constraint activation on the minimum distance from the Sun and by a single coasting phase. This behavior is illustrated in Fig. 13 that shows the trajectory towards $r_2 = 100\,\mathrm{AU}$ with $a_{\oplus} = 1\,\mathrm{mm/s^2}$ along with the time history of the cone angle α. Figure 13(b) shows that the coasting phase, whose time length is 1.4 years, starts about 10 month after the departure. The escape condition ($\mathcal{E} = 0$) is obtained after 2.4 years from the launch.

Near minimum-time trajectories

So far, the electric sail has been employed during the whole trajectory length, with the only exception of the coasting phases. With the aid of Fig. 12, one concludes, for example, that the propelling system would be engaged for about 17 years if $a_{\oplus} = 1\,\mathrm{mm/s^2}$, or 11 years if $a_{\oplus} = 2\,\mathrm{mm/s^2}$ when $r_{\min} = 0.5\,\mathrm{AU}$. These high values of time intervals suggest to investigate
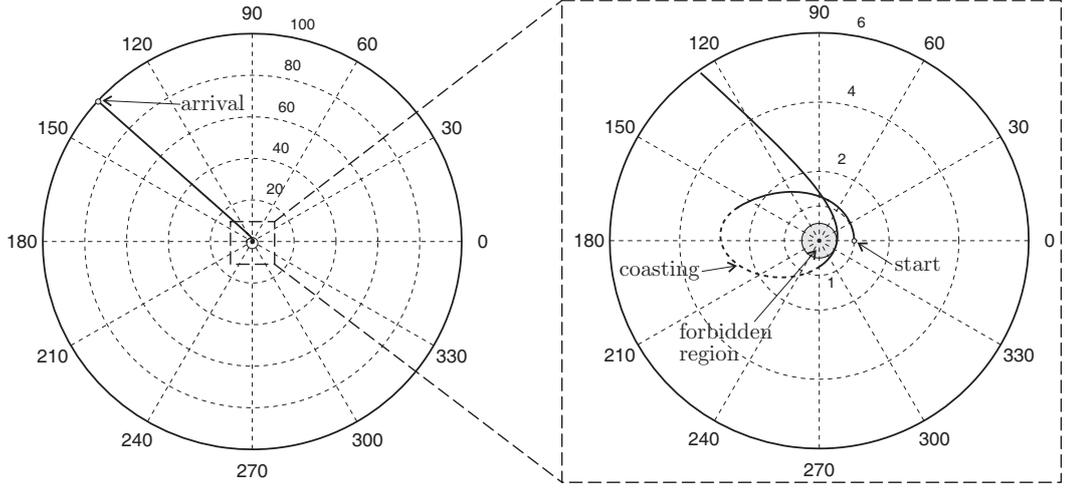
a) Optimal trajectory.
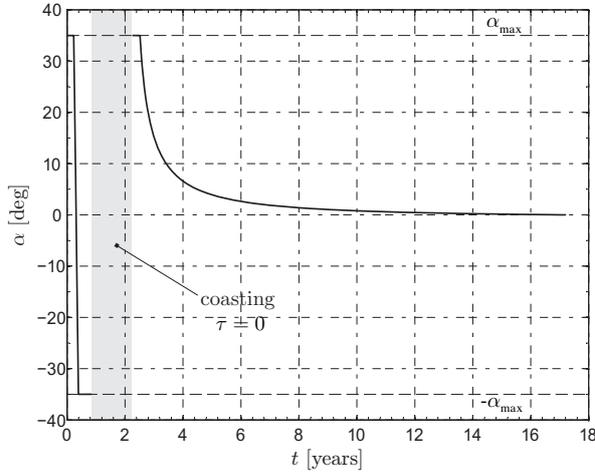
b) Sail cone angle vs. time.
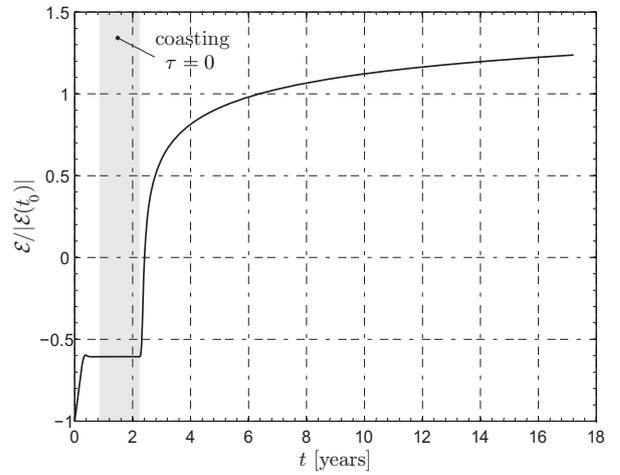
c) Mechanical energy vs. time.

Figure 13: **Minimum-time trajectory towards the heliosheath ($r_2 = 100\,\mathrm{AU}$) for $a_\oplus = 1\,\mathrm{mm/s^2}$ and $r_{\min} = 0.5\,\mathrm{AU}$.**

different (that is, not optimal) strategies to reach the heliosheath. An interesting alternative is obtained by observing that when SWA strategies are employed to approach the outer SS, the sailcraft covers a nearly rectilinear trajectory when r is greater than about 15 AU, see Fig. 13(a). Therefore, the spacecraft motion experiences an accelerated motion with a very low acceleration value whose modulus tends progressively to decrease as the sailcraft moves away from the Sun [see Eqs. (19)-(20)]. Assuming to switch off the propulsion system

during this nearly-rectilinear trajectory phase, one would obtain a slightly decelerated motion with a terminal velocity equal to the value of V_∞ attained when the thrust is set to zero. Actually, the simulations show that if one switches off the thrust at any point during the nearly-rectilinear trajectory phase, the sailcraft velocity is essentially equal to the hyperbolic excess speed corresponding to the osculating orbit calculated at the switching-off instant. Therefore, an alternative and near-minimum time strategy to reach high SS distances in a two-dimensional framework could be that of maximizing V_∞ for a given flight time (the latter value might be chosen by taking into account the propulsion system requirements and the mission constraints).

With such a strategy, the thrust may be switched off at t_2 and the sail may be jettisoned. Note that the problem of maximizing V_∞ for a given t_2 is nearly equivalent to that of minimizing the flight time necessary to reach a given hyperbolic excess speed with respect to the Sun system. Therefore, it is possible to use the previously discussed mathematical model with boundary constraints (5). In the following we confine our analysis to thrust-on times less than $10\,\mathrm{years}$ [42] and use moderate values of characteristic accelerations in the range $[0.6,\,1]\,\mathrm{mm/s^2}$. The simulation results are summarized in Fig. 14. For example, a characteristic acceleration $a_\oplus = 1\,\mathrm{mm/s^2}$ allows one to obtain a hyperbolic excess speed of about $7\,\mathrm{AU/year}$ at $r(t_2) \simeq 33\,\mathrm{AU}$ when $t_2 = 10\,\mathrm{years}$. Assuming that at $t = t_2$ the motion is rectilinear uniform with a velocity $V \triangleq \sqrt{u(t_2)^2 + v(t_2)^2}$ equal to V_∞ (see Fig. 15), the sailcraft would require $(100-33)/7 \simeq 9.6\,\mathrm{years}$ to reach the heliosheath distance $r_2 = 100\,\mathrm{AU}$ and the total mission time would be $(10+9.6) = 19.6\,\mathrm{years}$. As a comparison with an optimal trajectory, Fig. 12 shows that, using $r_{\min} = 0.5\,\mathrm{AU}$ and $a_\oplus = 1\,\mathrm{mm/s^2}$, the minimum flight time is about $17.2\,\mathrm{years}$. If, instead, one maximizes the hyperbolic excess velocity, the additional time necessary to reach the heliosheath distance is $2.4\,\mathrm{years}$, with an increase of $+14\%$ with respect to the minimum admissible value. However, the corresponding propulsion
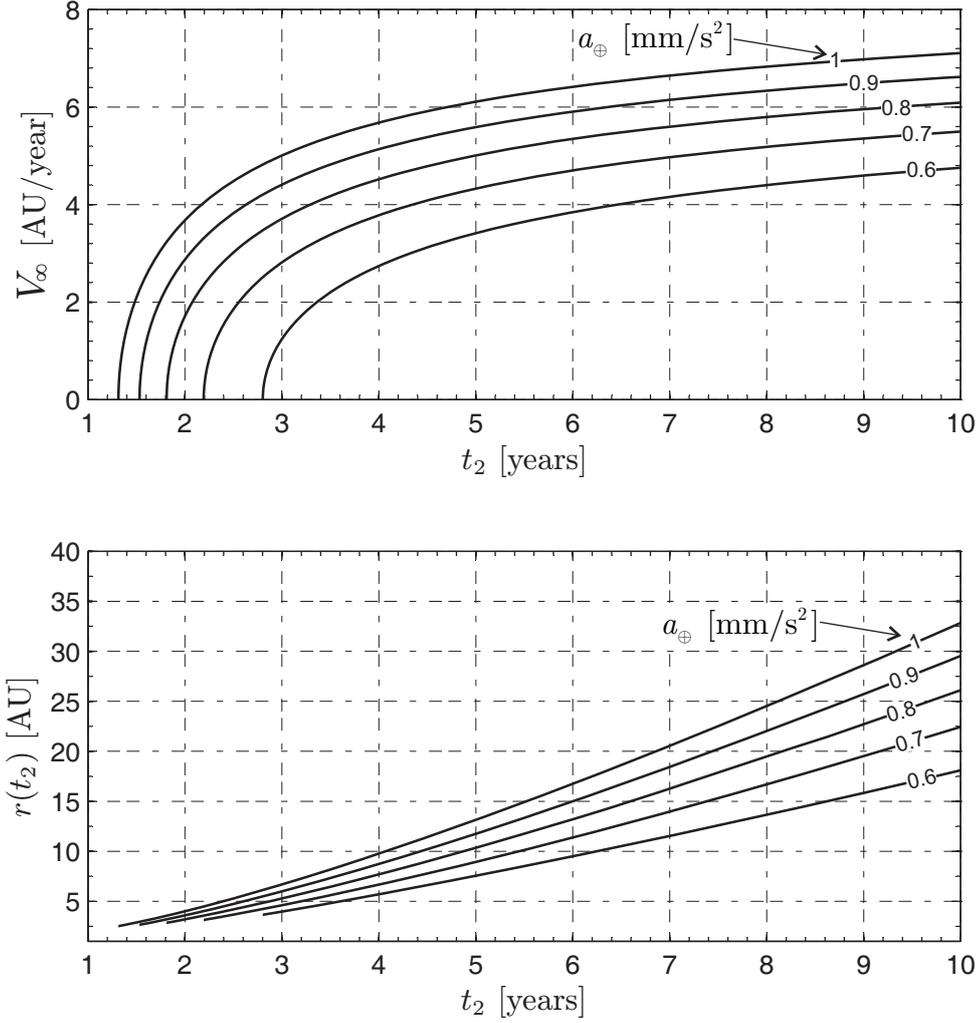
Figure 14: **Minimum time to reach a given V_∞ ($r_{\min} = 0.5\,\mathrm{AU}$).**

system engagement decreases dramatically from $17.2\,$years (in the minimum time case) to $10\,$years (in the maximum V_∞ case), with a percentage reduction of 42%.

When a near minimum-time strategy is used, the electric sail performance is strongly influenced by the minimum admissible value of perihelion radius. In fact, the sailcraft tends to approach as much as possible the Sun to fully exploit the SWA effect and to maximize the hyperbolic excess velocity. This behavior is better appreciated with the aid of Fig. 16, in which the influence of $r_{\min}$ on the flight time is shown for different values of the hyperbolic excess speed when $a_\oplus = 1\,\mathrm{mm/s^2}$. Note that the mission times are made dimensionless with
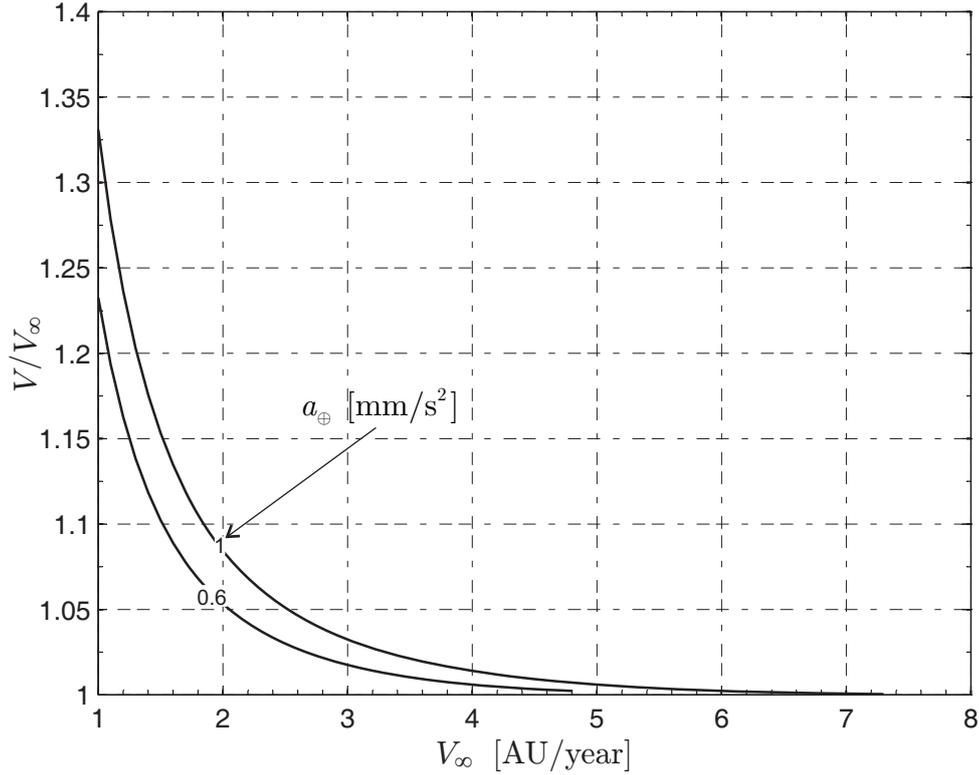
Figure 15: Final sailcraft speed as a function of V_∞ and $a_\oplus$ ($r_{\min} = 0.5\,\mathrm{AU}$).

the values corresponding to $r_{\min} = 0.5\,\mathrm{AU}$ (the latter may be taken from Fig. 14).

Using the data from Fig. 16, if one uses $r_{\min} = 0.33\,\mathrm{AU}$ (copper tethers), a sailcraft hyperbolic excess velocity of $V_\infty = 7\,\mathrm{AU/year}$ is reached within a time length equal to 63% the time necessary to obtain the same V_∞ with $r_{\min} = 0.5\,\mathrm{AU}$ (aluminium tethers). Because a hyperbolic excess of $7\,\mathrm{AU/year}$ requires $10\,\mathrm{year}$ when $a_\oplus = 1\,\mathrm{mm/s^2}$ and $r_{\min} = 0.5\,\mathrm{AU}$ (see Fig. 14) a closer approach to the Sun, up to $0.33\,\mathrm{AU}$, guarantees a mission time decrease of about $3.7\,\mathrm{year}$. Similar conclusions can be obtained in terms of final solar distance $r(t_2)$.

Three-Dimensional Trajectories Towards the Heliosheath

The previous analysis, under the simplified assumption of a two-dimensional problem, provides a first order estimate of the minimum performance (in terms of characteristic acceleration) required by the electric sail to either attain a flyby with an outer planet or to reach
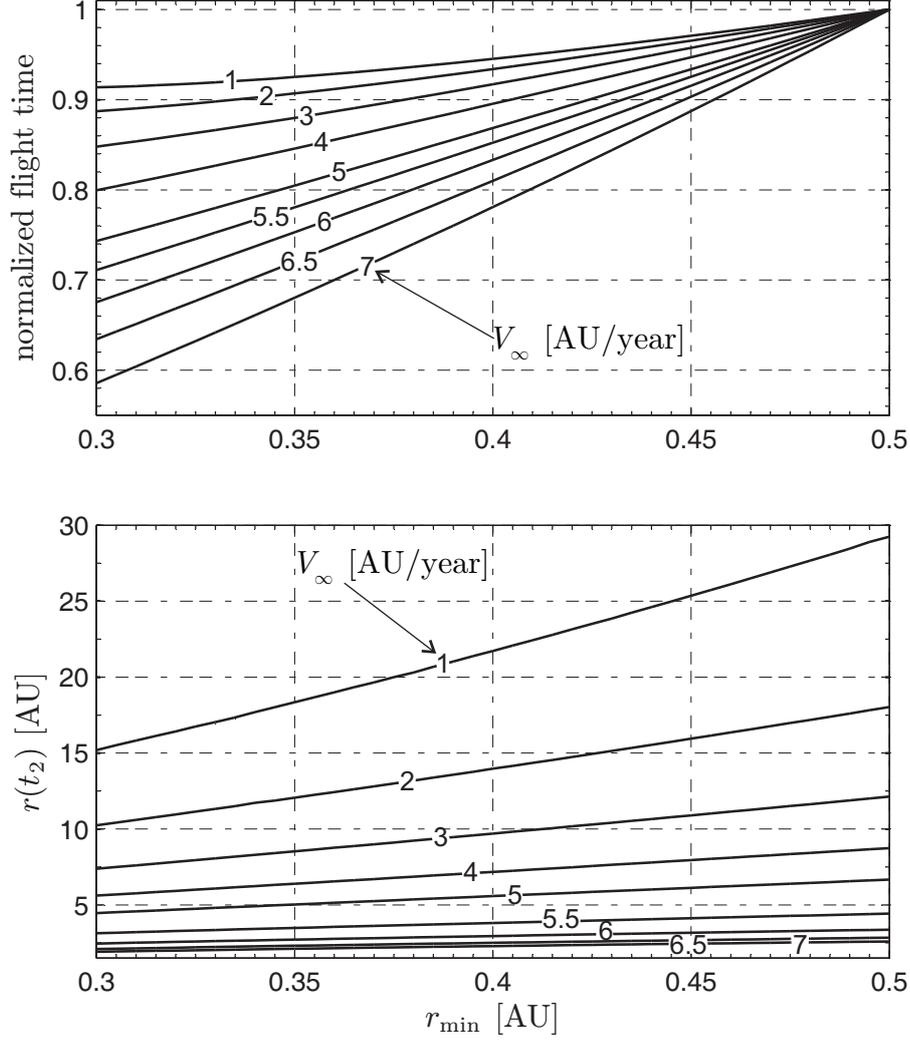
Figure 16: Flight time and final solar distance as a function of $r_{\min}$ and V_∞ when $a_\oplus = 1\,\mathrm{mm/s^2}$.

the boundaries of the SS (that is, distances on the order of 100 AU) in a given time interval t_2. In this section we will investigate transfers towards the heliosheath and the heliopause by taking into account the three-dimensionality of the actual electric sail trajectory. In fact, both the heliosphere and the heliosheath are shaped by the interaction of the solar wind with the local interstellar medium, such as the Earth's magnetosphere is droplet shaped by the solar wind [7]. Currently, the ecliptic latitude and longitude of the heliosheath nose are given by $\phi_H = 7.5\,\mathrm{deg}$ and $\psi_H = 254.5\,\mathrm{deg}$, respectively.

Because the sailcraft longitude at the final instant t_2 is strictly connected to its initial

position on the departure orbit, the previously estimated mission times are certainly less than that achievable with a truly three-dimensional trajectory. To quantify such differences, the mathematical problem must be slightly changed with the introduction of a suitable inertial spherical reference system $\mathcal{T}_\odot(r, \psi, \phi)$, where ψ is the ecliptic longitude and ϕ is the ecliptic latitude, see Fig. 17. The orbital reference frame $\mathcal{T}_L(x_L, y_L, z_L)$, illustrated in Fig. 17, is
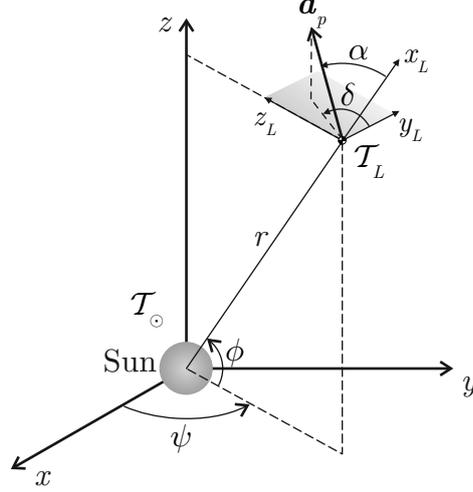
Figure 17:   Spherical reference frame.

useful to express the direction of the propelling acceleration vector $\boldsymbol{a}_p$ through the cone angle $\alpha \in [0, \alpha_{\max}]$ and the clock angle $\delta \in [0, 2\pi]$. The latter, defined in analogy with the solar sail literature [32, 43–45] as the angle between y_L and the projection of $\boldsymbol{a}_p$ in the plane (y_L, z_L), points out the propelling thrust angle in the plane perpendicular to the Sun-sailcraft direction. In particular, the propelling acceleration components are given by

$$[\boldsymbol{a}_p]_{\mathcal{T}_L} = a_\oplus \, \tau \, \left(\frac{r_\oplus}{r}\right)^{7/6} \begin{bmatrix} \cos\alpha \\ \sin\alpha \, \cos\delta \\ \sin\alpha \, \sin\delta \end{bmatrix} \tag{11}$$

The electric sail equations of motion and the corresponding Euler-Lagrange equations are here omitted for the sake of conciseness. The interested reader is referred to Ref. [24] for

a detailed discussion of those equations along with the optimal control law involving the three control variables τ, α, and δ. The equations of motion and the control law discussed in Ref. [24] are directly applicable to the problem at hand as long as the constraint on the minimum solar distance is inactive. When, instead, such a constraint on $r_{\min}$ is activated, in analogy with the previous two-dimensional problem, the trajectory is divided into two parts. The enforcement of the transversality condition at the point where the two sub-trajectories are joined, prescribes that all of the state variables and Euler-Lagrange variables are continuous in the time interval $[t_0, t_2]$ with the exception of λ_r. In fact, the latter displays a jump in correspondence of the unknown time instant t_1. In particular, when the constraint on $r_{\min}$ is active, the optimal trajectory is tangent to a sphere centered at the Sun and with radius equal to $r_{\min}$. Therefore, in analogy to Eqs. (9), the two scalar conditions to be met at t_1 are $r(t_1) = r_{\min}$ and $u(t_1) = 0$.

Contrary to the planar case, in a three-dimensional space the cylindrical symmetry of the problem is lost. This happens even for a circular initial orbit (recall that the Earth's orbital eccentricity has a negligible effect on the mission time), because of the existence of a preferential direction in the space. The latter coincides with the line joining the Sun with the heliopause nose and is characterized through ψ_H. In mathematical terms the starting sailcraft longitude $\psi_0 \triangleq \psi(t_0)$ is an unknown of the problem, whose value may be found by imposing the final condition $\psi(t_2) = \psi_H$. Finally, the total mission time t_2 is found by enforcing the transversality condition (6), while the initial value of λ_ϕ is obtained through the condition $\phi(t_2) = \phi_H$ at the final time.

Taking into account the results obtained with the previous two-dimensional analysis, see Fig. 12, to quantify the performance decrease connected to the actual three dimensional trajectory shape, minimum time trajectories towards the heliosheath nose have been studied assuming a minimum distance $r_{\min} = 0.5\,\mathrm{AU}$, an initial circular orbit with radius equal to

1 AU, and a characteristic acceleration ranging in the interval $a_\oplus \in [1, 2]\,\text{mm/s}^2$. In all of these simulations the propelling thrust is assumed to be available for the whole mission time and, using the results for the two-dimensional case, the constraint on the minimum distance is set active. The variation of the flight time t_2 with $a_\oplus$ is illustrated in Fig. 18(a) where the flight time corresponding to the two-dimensional case is displayed for comparison (see also Fig. 12).

Figure 18(a) shows the increase of t_2 in the transition from the two-dimensional to the three-dimensional case. Such an increase varies between 5% and 15% for electric sails with medium-high performance ($a_\oplus \in [1.2, 1.8]\,\text{mm/s}^2$) and tends to reduce with an increase of the characteristic acceleration. For example, when $a_\oplus = 2\,\text{mm/s}^2$, the difference in flight time for the two models is only 5 months, that is, less than 3.5% of the total mission time. Figure 18(a) also shows that the two-dimensional analysis is unsuitable for characteristic accelerations on the order of (or less than) $a_\oplus = 1\,\text{mm/s}^2$, when the differences exceed 26%. Such a behavior may be explained by observing that the required variation of the orbital plane takes place during the approaching phase to the Sun and soon after the SWA, when the propelling acceleration attains its maximum value. Unlike the two-dimensional case, the propelling acceleration is used, in part, to vary the value of ϕ instead of increasing the sailcraft specific mechanical energy. This reduced capability of exploiting the SWA in a three dimensional trajectory increases with a decrease of $a_\oplus$, and is ultimately responsible of the growing differences in mission times between the two models.

Figure 18(b) shows the variation in initial sailcraft longitude ψ_0 with $a_\oplus$. The information on the value of ψ_0 allows one to estimate the sailcraft launch window. Because the position of the heliosheath nose is nearly independent of time, the launch window obtainable from Fig. 18(b) repeats every year.

As outlined in the two-dimensional analysis, the use of an electric sail for the whole
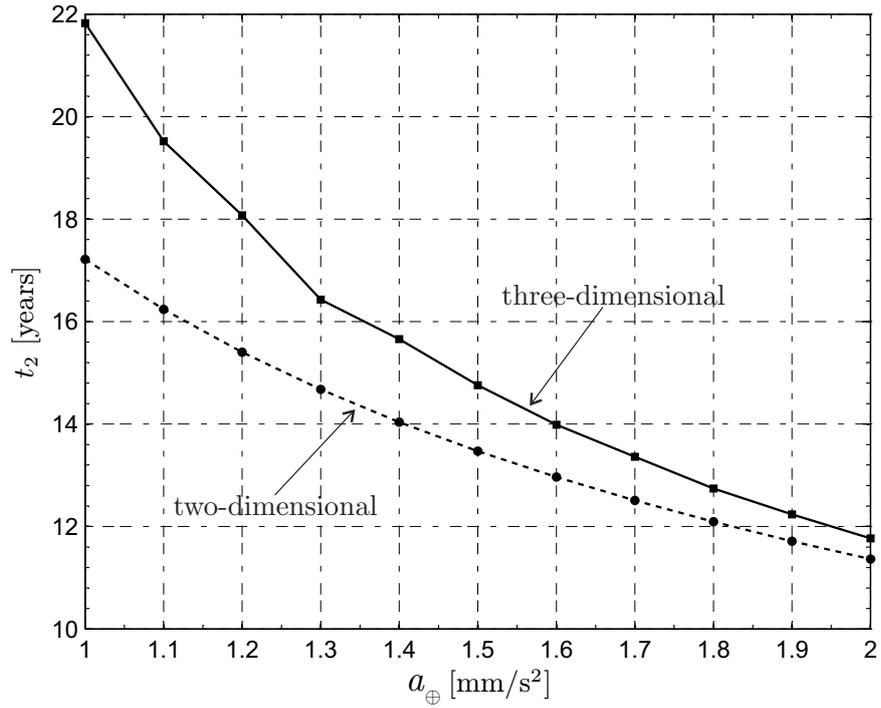
a) Flight time.
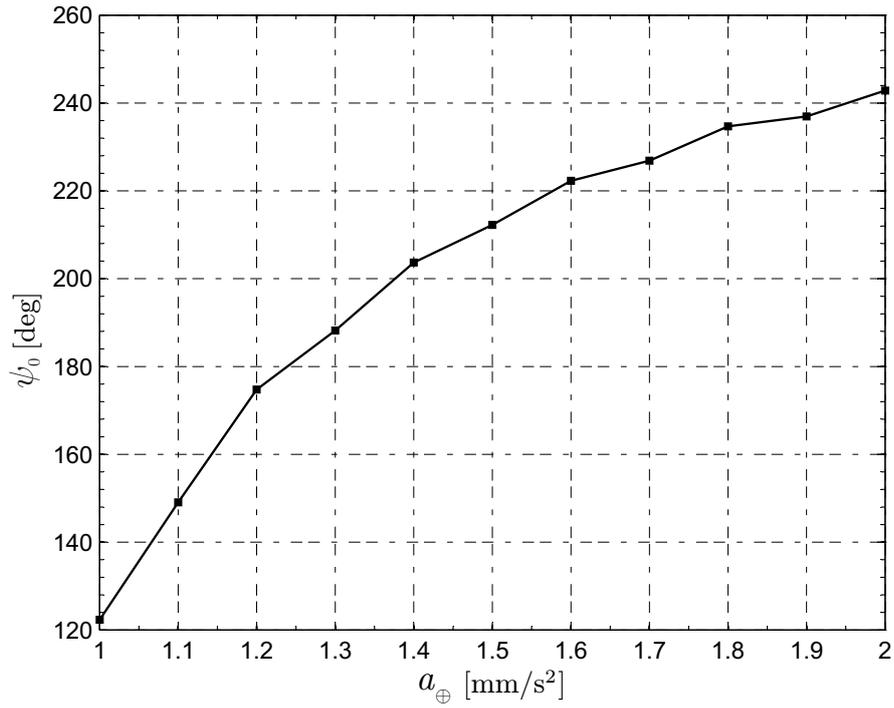
b) Initial heliocentric longitude.

Figure 18: Mission performance towards the heliosheath nose with $r_{\min} = 0.5\,\mathrm{AU}$.

mission time implies that the propulsion system must operate for a time length of 10-20 years, depending on the value of $a_\oplus$. Because the modulus of the propelling acceleration decreases sharply with the Sun's distance (for example $a_p/a_\oplus \simeq 6.8\%$ when $r = 10\,\text{AU}$), it is possible to imagine a mission strategy in which the sail is jettisoned at a distance r_c. Such a strategy, similar to what was studied by Sauer in Ref. [4] for solar sails, plans a flight by inertia between r_c and r_2, thus simplifying the acquisition of science data without any interference with the sail. Using such a mission strategy, a number of new trajectories towards the heliosheath nose have been simulated. In accordance to Sauer [4], and to obtain a direct comparison with solar sails, a cutoff distance of $r_c = 5\,\text{AU}$ was enforced in the simulations. Also, only solutions with flight times less than 20 years have been considered. The simulation results, using three possible values of minimum solar distance $r_{\text{min}} = (0.33,\ 0.4,\ 0.5)\,\text{AU}$, are summarized in Fig. 19. A mission towards the heliosheath with $r_c = 5\,\text{AU}$ and a flight
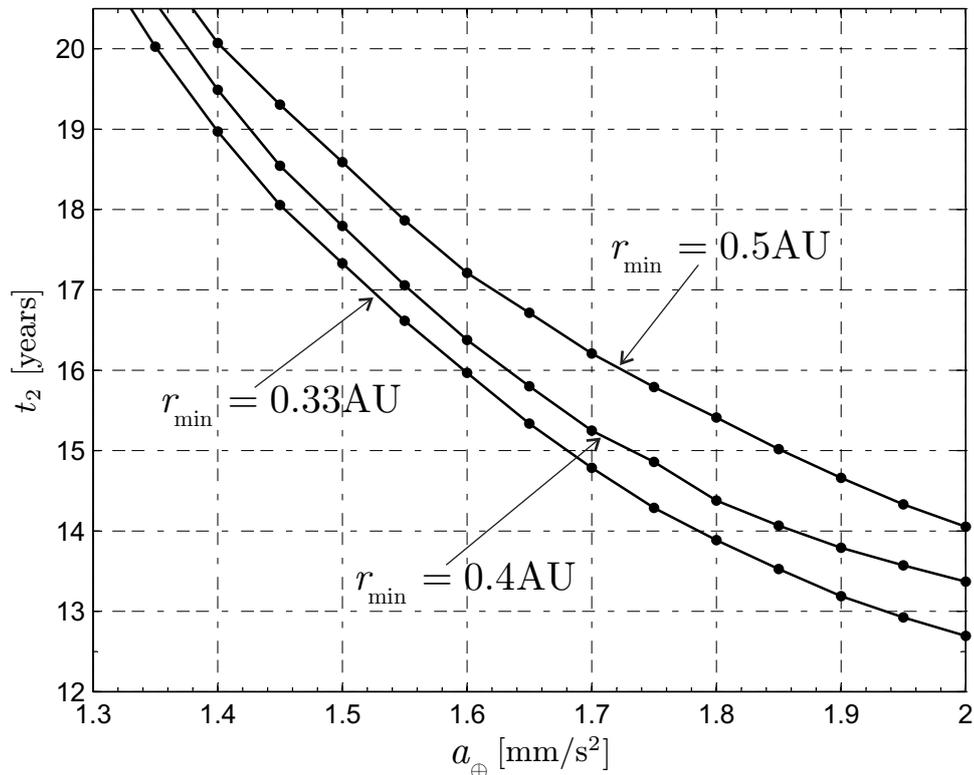
Figure 19:   Flight time for missions towards heliosheath nose with $r_c = 5\,\text{AU}$.

time less than 20 years requires, in the most favorable case ($r_{\min} = 0.33\,\mathrm{AU}$), a characteristic acceleration of at least $1.35\,\mathrm{mm/s^2}$. Moreover, using the results from Ref. [4] for comparative purposes, one observes that, the minimum perihelion distance being equal ($r_{\min} = 0.4$), the electric sail and the solar sail present similar performance for $a_\oplus \simeq 2\,\mathrm{mm/s^2}$, whereas for smaller values of characteristic acceleration a solar sail is definitely superior to an electric sail. The reason is that a solar sail has a more pronounced thrust increase with respect to an electric sail in the nearness of the perihelion (recall that for a solar sail the thrust varies as $1/r^2$). On the other hand an electric sail produces an higher thrust for distances $r > r_\oplus$, but such an advantage is reduced by the constraint on r_c.

It is interesting to investigate the influence of r_c on the mission time t_2. Assuming $r_{\min} = 0.5\,\mathrm{AU}$ and varying the cutoff distance in the range $r_c \in [5,\,30]\,\mathrm{AU}$, which corresponds to jettison the sail at a Sun's distance between Jupiter and Neptune, one obtains the results shown in Fig. 20. When the sail is jettisoned at a distance greater than $15\,\mathrm{AU}$, it is possible to reach the heliosheath nose in less than 20 years using characteristic accelerations that do not exceed $1.3\,\mathrm{mm/s^2}$. Alternatively, if one uses a sufficiently high characteristic acceleration, say $a_\oplus = 1.5\,\mathrm{mm/s^2}$, and assuming $r_c = 15\,\mathrm{AU}$, one obtains a time saving of more than 2.5 years with respect to the case in which the sail is jettisoned at a distance of $5\,\mathrm{AU}$ from the Sun. Clearly, as r_c is increased, the sail operating time length $t_c \triangleq t(r = r_c)$ increases as well, as is shown in Fig. 21. Such a time length will now be referred to as sailing mode time. We explicitly note that t_c does not, in general, coincide with the time length t_{on} in which the sail produces a thrust ($\tau = 1$), because the optimal trajectory may include the presence of coasting arcs. In other terms $t_c \geq t_{\mathrm{on}}$, and the equality sign takes place only provided that the trajectory displays no coasting arcs. Therefore, from Fig. 21 one deduces that if $r_c < 30\,\mathrm{AU}$ and $a_\oplus > 1.2\,\mathrm{mm/s^2}$ the time t_{on} is less than 6 years, that is, is much less than the lifetime of 10 years conjectured in Ref. [42]. The hyperbolic excess speed V_∞ varies, in its
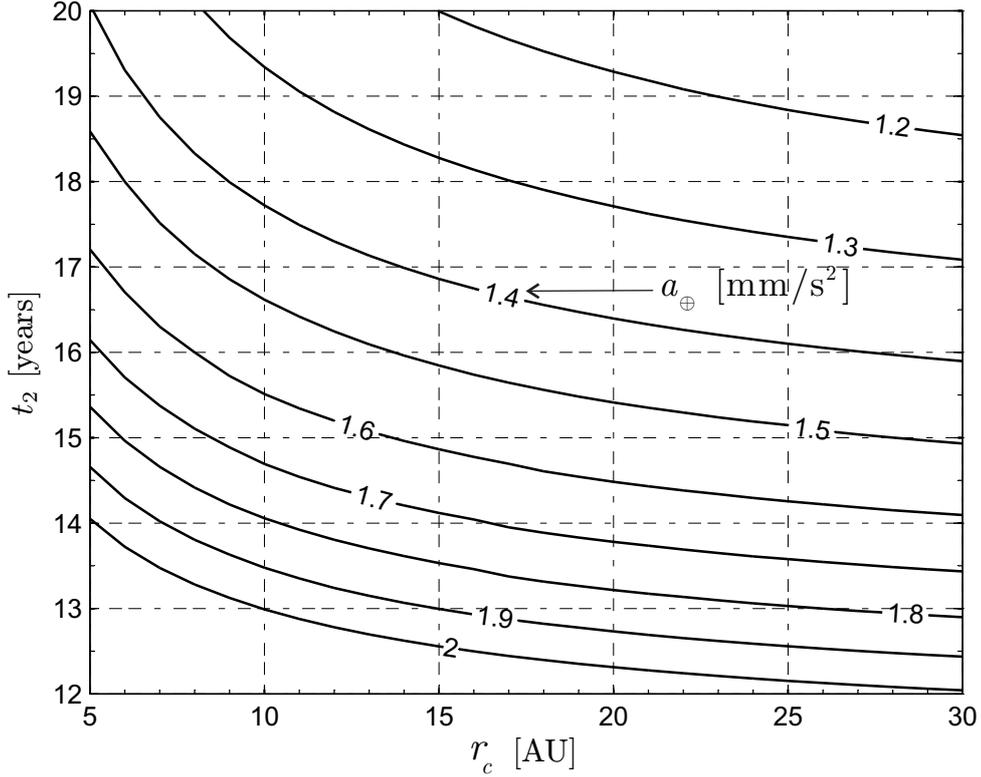
Figure 20: **Flight time for missions toward heliosheath nose ($r_{\min} = 0.5\,\mathrm{AU}$) as a function of r_c.**

turn, with r_c, as is shown in Fig. 22, and is less than $10\,\mathrm{AU/years}$ in all of the simulations. The value of V_∞ is a particularly important datum if one considers a possible extension for a mission originally planned to reach the heliosheath nose. This matter is further discussed in the next section.

Electric Sail as a Propulsion Option for the Interstellar Heliopause Probe

From our previous analysis it is apparent that an electric sail with a characteristic acceleration of about $2\,\mathrm{mm/s^2}$ may represent an interesting alternative to the conventional propulsion systems and to the solar sails for a mission towards the boundaries of the SS. In particular, our aim is now to investigate whether an electric sail may be considered as a potential primary propulsion system for a particular mission such as the Interstellar Heliopause
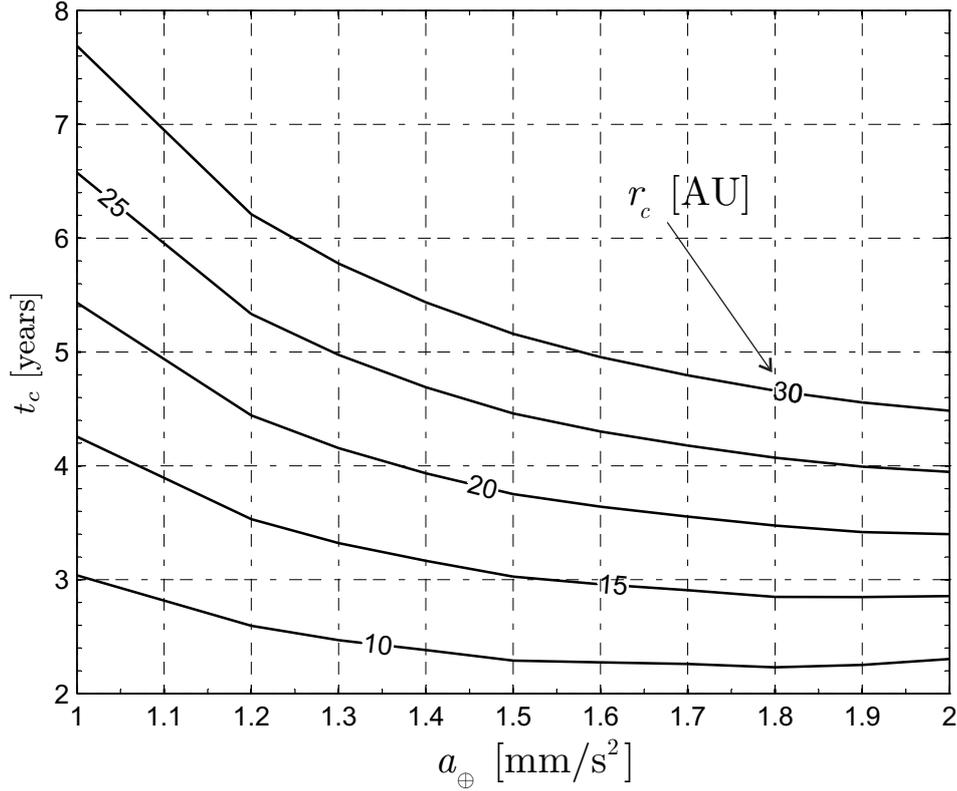
Figure 21:   Sailing mode time t_c as a function of r_c and $a_\oplus$ ($r_{\min} = 0.5\,\mathrm{AU}$).

Probe (IHP) [7, 30, 46]. This mission is one of the four Technology Reference Studies [6] introduced by the Planetary Exploration Studies Section of the Science Payload & Advanced Concept Office at ESA.

The IHP primary scientific aim [7] is that of analyzing the heliopause and the interstellar medium through in situ measurements with a highly miniaturized and a highly integrated payload suite [6]. Preliminary studies [7, 46] have estimated that the payload suite, with a mass of about 20 kg, can be accommodated inside a small spacecraft (the spacecraft platform) having an overall mass of $m_p = 213\,\mathrm{kg}$. Such a platform, equipped with a suitable propulsion system, should be able to reach the heliopause ($r_2 = 200\,\mathrm{AU}$) within 25 years of transfer time [46]. Three primary propulsion systems have been examined so far, chemical propulsion, nuclear electric propulsion and solar sailing. A solar sail was the only solution capable of meeting all of the mission requirements [6], especially as far as the total mission
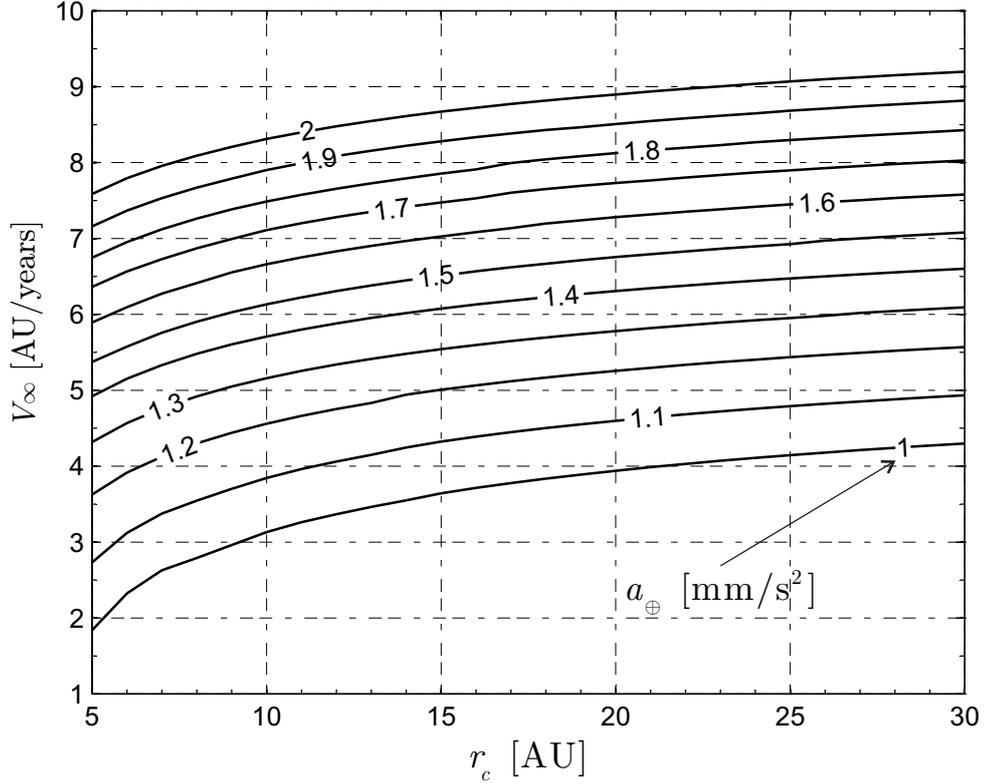
Figure 22: **Hyperbolic excess speed as a function of r_c and $a_\oplus$ ($r_{\min} = 0.5\,\mathrm{AU}$).**

time is concerned. In addition, the current conception of IHP mission requires that the primary propulsion system (that is, the solar sail) is jettisoned at a solar distance of 5 AU. As discussed above, this choice simplifies the scientific measurements avoiding any interference with the sail and, at the same time, reduces the propulsion system operating time, thus reducing the mission failure probability.

Before analyzing such a mission towards the heliopause nose in an optimal framework, we use the previous simulations to obtain an approximate estimate of the required electric sail performance. To this end, under the assumption of Keplerian motion (this is the case if the sail is jettisoned at a distance r_c from the Sun) the sailcraft attains its cruise phase with a uniform rectilinear motion at a distance $r \simeq 100\,\mathrm{AU}$ and with a velocity equal to V_∞. Let t_{100} be the time length necessary to reach the heliosheath nose (see Fig. 20). Observing that the further distance required by the sailcraft to pass from the heliosheath to the outer

boundary of heliosphere is about $\Delta r = 100 \, \mathrm{AU}$, the minimum required flight time can be approximated as:

$$t_2 \simeq t_{100} + \frac{\Delta r}{V_\infty} \qquad (12)$$

Because t_{100} and V_∞ are both functions of $a_\oplus$ and r_c, see Figs. 20 and 22, the flight time t_2 can be expressed in graphical form as shown in Fig. 23. Note that the data shown in the figure correspond to $r_{\min} = 0.5 \, \mathrm{AU}$. A slightly reduced value of t_2 could be obtained by decreasing the constraint on $r_{\min}$. From Fig. 23 and Eq. (12) one obtains that a mission towards the
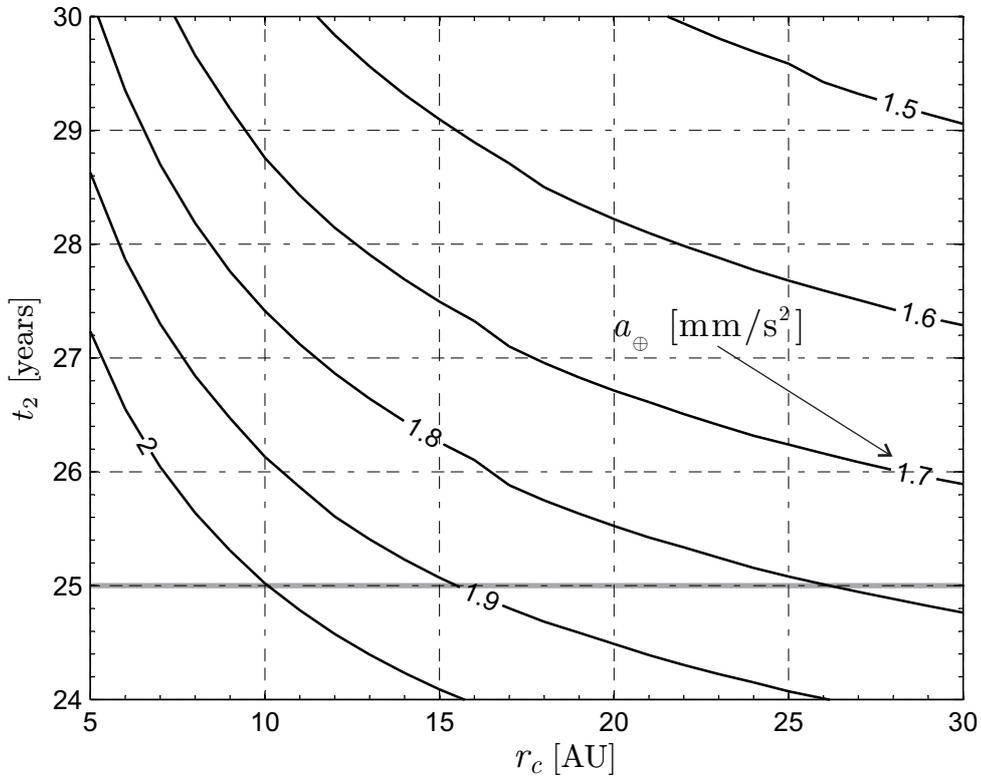
Figure 23: **Approximated flight time for missions towards the heliopause nose** ($r_2 = 200 \, \mathrm{AU}$) **with** $r_{\min} = 0.5 \, \mathrm{AU}$.

heliopause with the constraint of not exceeding 25 years of flight time and with a sail jettison at a distance less than 30 AU would require an electric sail with a characteristic acceleration not less than $1.8 \, \mathrm{mm/s^2}$. Also, unlike the solar sail option [7, 46], an electric sail jettison at a distance of 5 AU is unfeasible unless one tolerates much higher values of characteristic

acceleration. In practice, from Fig. 23, the minimum tolerable distance at which an electric sail could be jettisoned is approximately 10 AU, a distance comparable to that of Saturn.

Using three reasonable values of characteristic acceleration, that is, $a_\oplus = (1.8,\ 1.9,\ 2)\,\mathrm{mm/s^2}$, and estimating the jettison distance r_c from Fig. 23, the minimum time trajectory towards the heliopause ($r_2 = 200\,\mathrm{AU}$, $\psi(t_2) = \psi_H$, and $\phi(t_2) = \phi_H$) has been found by solving an optimal control problem, as previously discussed. The results corresponding to the three simulations have been summarized in Table 2. All of the three cases give the same launch

$a_\oplus$ [mm/s^2]	r_c [AU]	ψ_0 [deg]	t_1 [yrs]	t_c [yrs]	t_2 [yrs]	t_{on} [yrs]	V_∞ [AU/yr]
1.8	26	189.4	0.935	4.19	24.99	3.69	8.31
1.9	15	190	1.034	2.87	24.97	2.28	8.32
2.0	10	190.2	1.157	2.34	24.9	1.66	8.36

Table 2:   **Mission towards the heliopause ($r_2 = 200\,\mathrm{AU}$) with $r_{\min} = 0.5\,\mathrm{AU}$.**

window (ecliptic longitude $\psi_0 \simeq 190\,\mathrm{deg}$) and provide nearly the same value of hyperbolic excess speed $V_\infty \simeq 8.3\,\mathrm{AU/year}$. This result is in agreement with the data shown in Fig. 22. From Table 2, the time t_{on} during which the electric sail operates is, in the worst case with $a_\oplus = 1.8\,\mathrm{mm/s^2}$, slightly superior to 3.5 years. By comparing the value of t_{on} with that of t_c (the latter being taken from Fig. 21), one deduces that in the interval $t \in [t_0,\ t_c]$ the optimal trajectory displays at least one coasting phase. A more detailed analysis has revealed that in all of the simulation cases, such a coasting phase is actually unique and stops shortly before the reaching of the perihelion, at a distance of 0.5 AU from the Sun. The coasting phase and the time history of the state variables are shown in Fig. 24, which illustrates the simulation results corresponding to $a_\oplus = 2\,\mathrm{mm/s^2}$. For the sake of clearness, the time scale is confined to 2.5 years from the departure. From Fig. 24, as previously discussed, the change of latitude takes place in the first trajectory phase and the escape conditions are met after 1.2 years from the departure. The three-dimensional trajectory and its projection on the ecliptic plane are
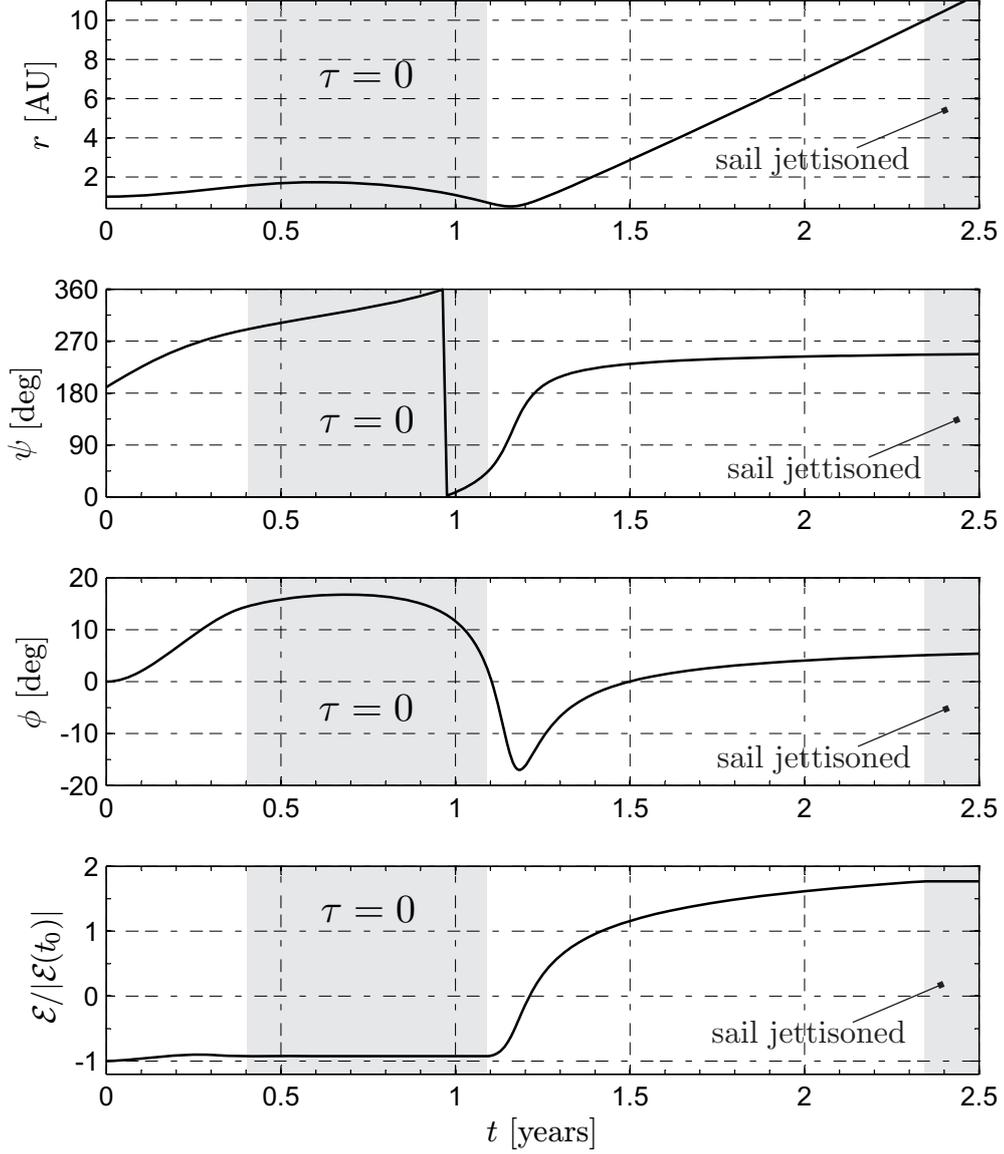
Figure 24: State parameters time histories for a mission towards the heliopause $(r_{\min} = 0.5\,\mathrm{AU}$ **and** $a_\oplus = 2\,\mathrm{mm/s^2}$**).**

shown in Fig. 25. The time history of the three control variables (τ, α, and δ) are summarized in Fig. 26 in which the sail jettison distance ($r_c = 10\,\mathrm{AU}$) and the sailcraft initial angular position $\psi_0 \simeq 190\,\mathrm{deg}$ are both highlighted.

Sailcraft mass budget

Having found the electric sail performance in terms of characteristic acceleration required to reach the heliopause nose within the prescribed time interval (about 25 years), it is now
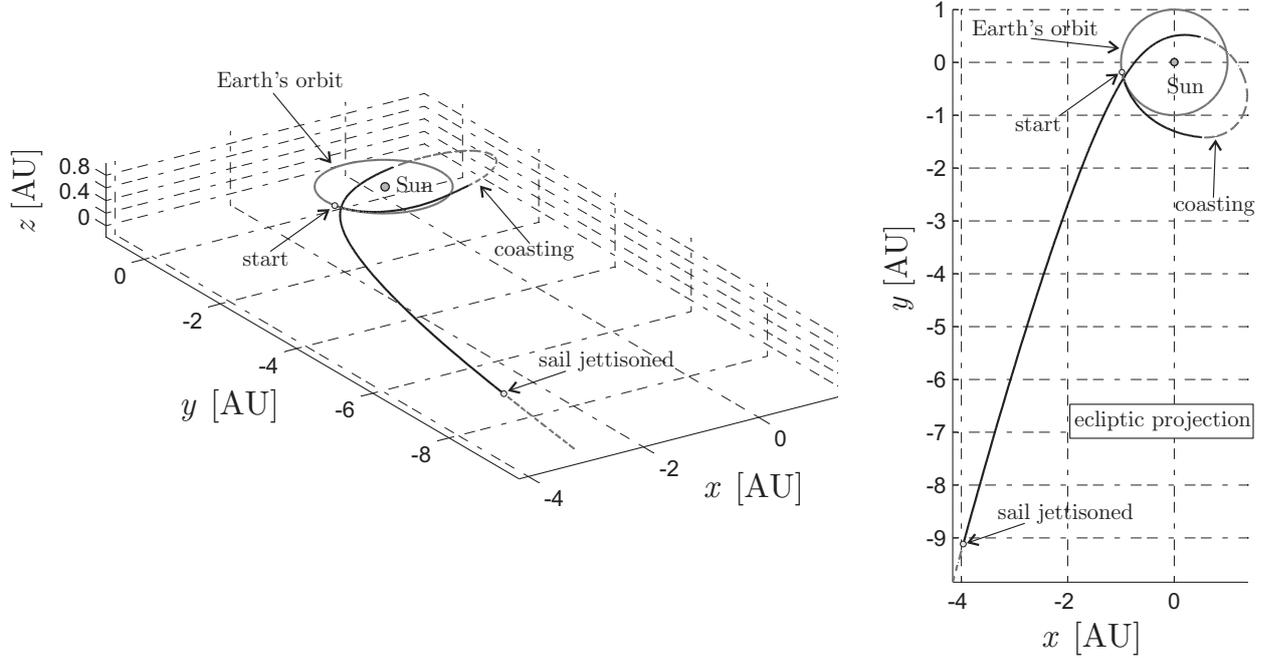
Figure 25: First part of the transfer trajectory towards the heliopause ($r_{\min} = 0.5\,\text{AU}$ and $a_{\oplus} = 2\,\text{mm/s}^2$).

necessary to investigate the corresponding requirements in terms of sailcraft mass budget for the IHP mission. In accordance to Ref. [7], it is possible to ideally subdivide the sailcraft into two subsystems based on the two main operational phases: a spacecraft platform, with total mass m_p, and an electric sail propulsion system with total mass m_E. Accordingly, the sailcraft in-flight initial total mass m_0 is given by:

$$m_0 = m_p + m_E \tag{13}$$

Because the platform mass value is given, that is, $m_p = 213\,\text{kg}$ [46], the calculation of m_0 requires an estimate of m_E. To this end we make use of a mathematical model taken from Ref. [22], which allows one to obtain a reasonable approximation of the total mass of an electric sail spacecraft and of its characteristic acceleration. The model proposed in Ref. [22] is based on the preliminary plasma simulations performed by Janhunen, the electric sail
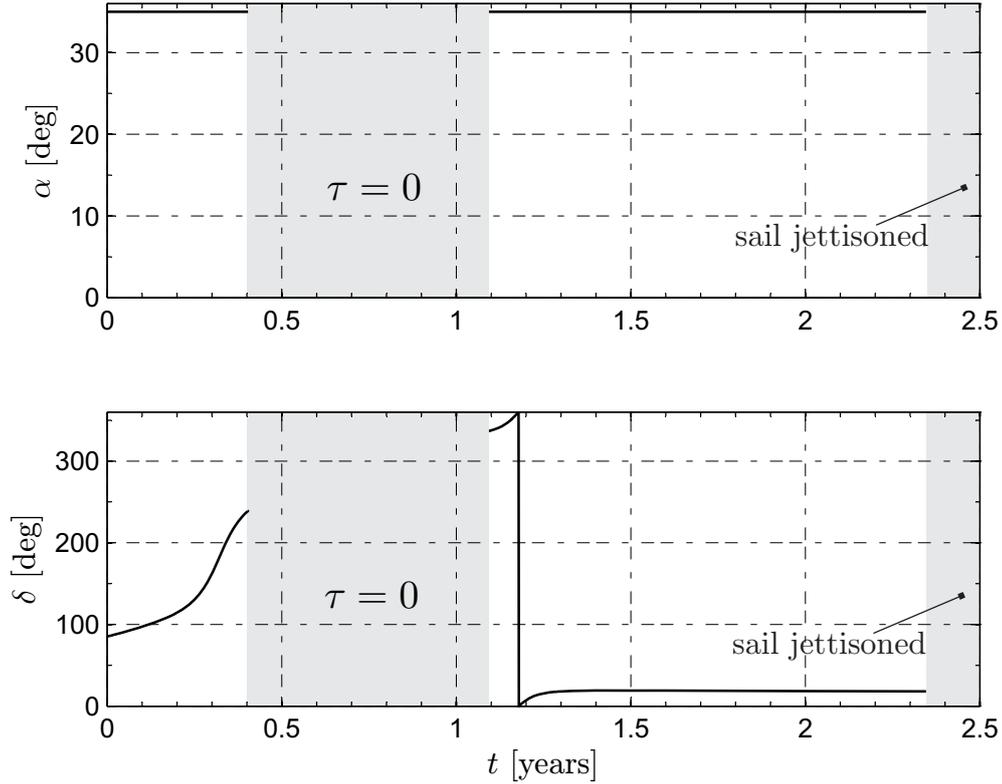
Figure 26: Controls time histories for a mission towards the heliopause ($r_{\min} = 0.5\,\text{AU}$ and $a_\oplus = 2\,\text{mm/s}^2$).

inventor, and published in Ref. [20]. In the light of the currently available information, those plasma simulations seem to provide excessively conservative results. In fact, the propelling thrust obtainable by the electric sail depends on the number of electrons that are trapped by the potential structures of the tethers, because such electrons tend to shield the charged tethers and reduce their effect on the solar wind. Very recent studies have conjectured the existence of a natural mechanism that tends to remove the trapped electrons [47]. Using this new model, the electric sail thrust per unit length of tether (σ_F) is roughly five times higher than what was originally reported in Ref. [20]. A preliminary application example for the new thrust model is given in Ref. [42]. In particular, an electric sail comprising a total of $n = 100$ tethers, each one being of $l = 20\,\text{km}$ length, in an average solar wind is capable of developing a maximum propelling thrust $F = 1\,\text{N}$ at a solar distance of $r = r_\oplus$.

In the example proposed in [42], the 20 kV charged tethers have a total mass of $m_{th} = 11$ kg. With such a configuration, the electron gun requires $P = 400$ W power to operate. Using these data as a reference, it is possible to obtain a first order estimate of the sailcraft mass distribution by suitably scaling the main contributions such as the electron gun power, the tethers total mass, and the propelling thrust. Let $L \triangleq n\,l = 2\,000$ km the total tethers length. Using the data from Ref. [42] one obtains

$$\sigma_F \triangleq \frac{F}{L} = 500\,\frac{\text{nN}}{\text{m}} \quad , \quad \sigma_{m_{th}} \triangleq \frac{m_{th}}{L} = 5.5 \times 10^{-6}\,\frac{\text{kg}}{\text{m}} \quad , \quad \sigma_P \triangleq \frac{P}{L} = 2 \times 10^{-4}\,\frac{\text{W}}{\text{m}} \quad (14)$$

The numerical values for σ_F, $\sigma_{m_{th}}$, and σ_P that appear in Eq. (14) are treated as design data per unit tether length, and will be used for estimating the total sailcraft mass of the IHP mission. In a preliminary mass breakdown calculation, the electric sail can be divided into three subsystems: the power system (with mass m_P), the tethers (with mass m_{th}) and all of the remaining elements that, for the sake of compactness, are comprised in the term "structure" (with mass m_s). The mass m_s includes, besides the sailcraft structural mass, the electron gun mass, the remote control mass, etc. Accordingly, the total mass of the electric sail can be written as:

$$m_E = k_P \underbrace{\frac{\sigma_P\,L}{\eta}}_{m_P} + k_s \left(\underbrace{\sigma_{m_{th}}\,L}_{m_{th}} + m_s \right) \qquad (15)$$

where now L, the total tethers length, is a design variable that must be calculated.

In Eq. (15) η is the specific power, that is, the power per mass unit associated to the power subsystem, while $k_P > 1$ and $k_s > 1$ are two dimensionless coefficients that model the uncertainty level (that is, the safety mass margins) in the definition of the sailcraft mass breakdown.

Taking into account the solar distance at which the sailcraft must operate, and in analogy

to a similar choice for the platform [46], the best option for the power subsystem is represented by a radio-isotope thermoelectric generator (RTG). Current RTGs [48] are characterized by a specific power of about $5\,\mathrm{W/kg}$, but it is expected that in a near future the specific power may be increased up to $10\,\mathrm{W/kg}$ [7]. The currently estimated [46] specific power needed by the IHP platform is of about $10\,\mathrm{W/kg}$.

Due to a sufficiently good knowledge of RTG technology, we assume a safety margin of 20%, that is, $k_P = 1.2$ in Eq. (15). On the other hand, the current scarce knowledge of the system details for the remaining parts of the electric sail implies a greater uncertainty level on k_s. A reasonable choice is to double the previous safety margin and assume, therefore, $k_s = 1.4$. To make a comparison, in the design of the IHP mission with a solar sail as the primary propulsion system, the safety margin was set equal to 20% [46].

Because the total electric sail thrust F at a distance of $r_\oplus$ is given by the product between the total length L and σ_F, from the definition of the characteristic acceleration and taking into accounts Eqs. (13)-(15), the following relationship is obtained:

$$a_\oplus \triangleq \frac{F}{m_0} = \frac{\sigma_F\, L}{m_p + k_P\, \sigma_P\, L/\eta + k_s\, (\sigma_{m_{th}}\, L + m_s)} \tag{16}$$

Recalling Eq. (14), Eq. (16) allows one to express the characteristic acceleration as a function of the three design parameters L, η, and m_s. Using the two values $\eta = (5,\ 10)\,\mathrm{W/kg}$, which correspond, as stated, to the current and near future technology level, it is possible to draw the function $a_\oplus = a_\oplus(L,\ m_s)$, as is shown in Fig. 27.

By comparing Figs. 27(a) and 27(b), $a_\oplus$ and L being equal, an increase of the specific power from 5 to $10\,\mathrm{W/kg}$ would allow one to increase the structural mass of about 50 kg. Alternatively, m_s and $a_\oplus$ being equal (the latter value being given by the mission requirements, see Tab. 2), the increase in η translates into a reduction of the total tethers
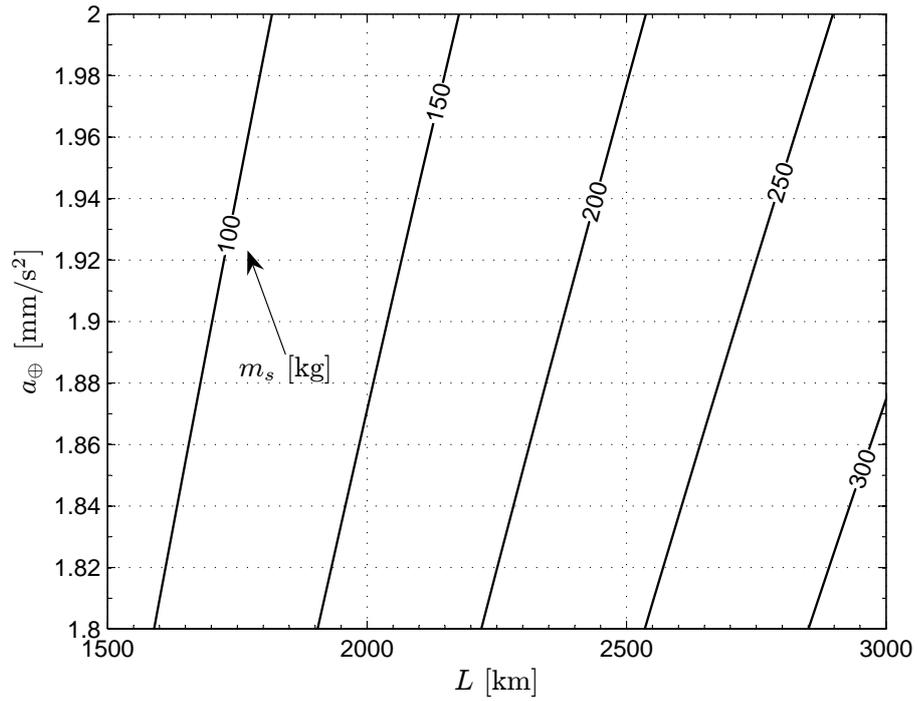
a) $\eta = 5\,\mathrm{W/kg}$
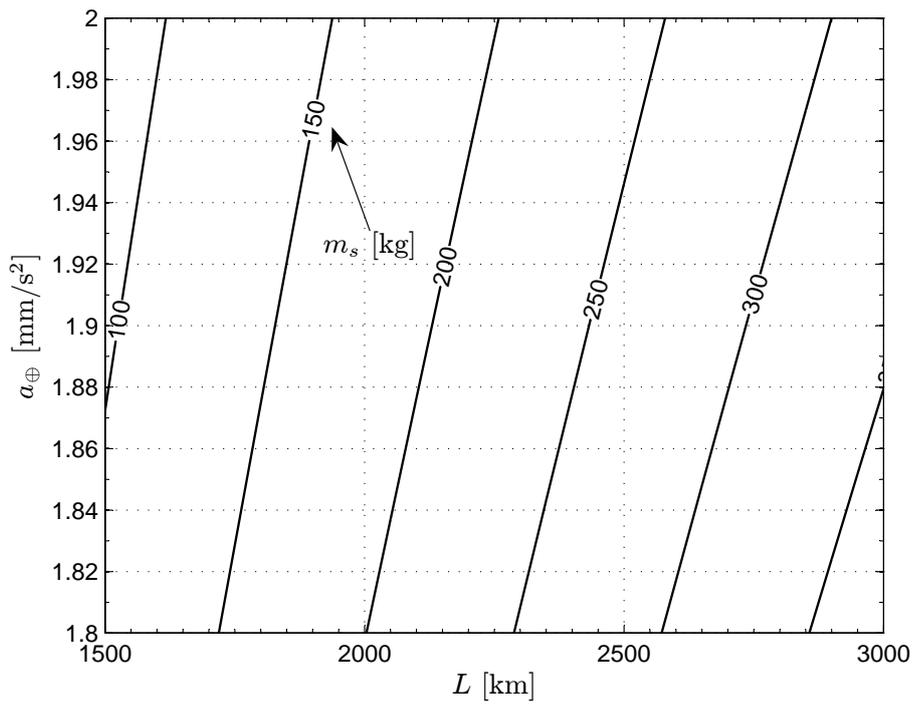
b) $\eta = 10\,\mathrm{W/kg}$

Figure 27: Characteristic acceleration as a function of total tethers length L and structure mass m_s.

length. For an electric sail the value of L is roughly an index of the system complexity, as the reflecting surface is for a solar sail. Therefore, an increase of the specific power would be a very desirable result. However, the corresponding obtainable reduction in the tethers length, using the currently available values of $a_\oplus$, would not exceed $200 - 300\,\mathrm{km}$, as is shown in Fig. 28, which corresponds to a percentage decrease of $10 - 15\%$ with respect to the value of L required by this mission typology. Assuming $L = 2500\,\mathrm{km}$ (that is, 25%
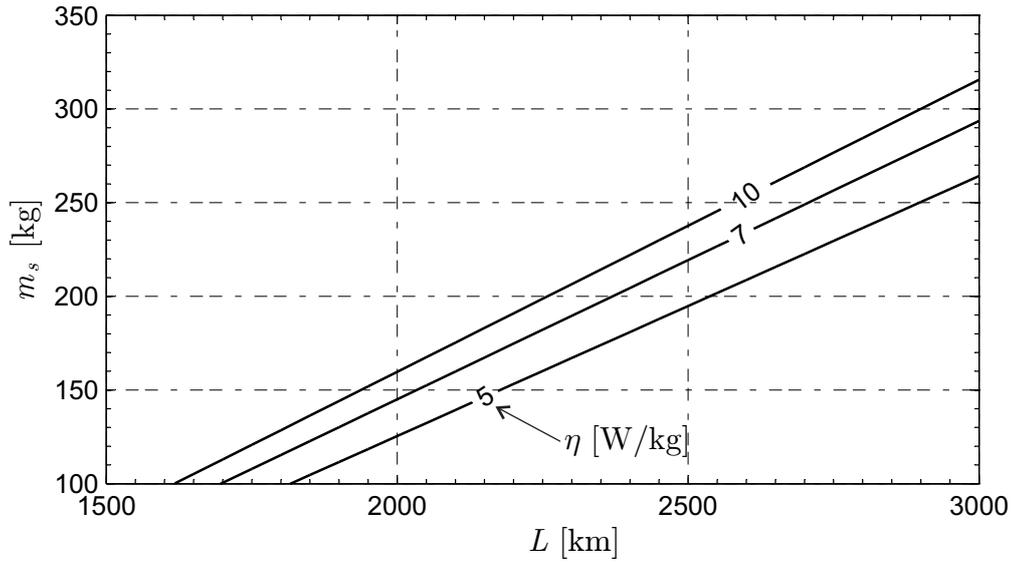
Figure 28: **Total tethers length L as a function of m_s and η for $a_\oplus = 2\,\mathrm{mm/s^2}$.**

greater than the value given in the example proposed in Ref. [42]), for each one of the three values of characteristic acceleration shown in Tab. 2, it is possible, with the aid of Eq. (16) and Fig. 27, to estimate the value of m_s and of the other sailcraft masses. The results of this calculation for $\eta = (5,\,10)\,\mathrm{W/kg}$ have been summarized in Table 3. Note that, once L is given, from the definition of σ_F the maximum propelling thrust at $1\,\mathrm{AU}$ is equal to $F = 1.25\,\mathrm{N}$. Table 3 shows that for all of the three cases the structure mass is comparable to that of the platform. If one thinks of the platform as a payload linked to the electric sail, the previous mass breakdown shows that an IHP mission sailcraft can carry a payload mass fraction between 30% and 35%. For example, using the data from Ref. [46], an IHP mission

Mass	$a_\oplus$=1.8 mm/s^2		$a_\oplus$=1.9 mm/s^2		$a_\oplus$=2 mm/s^2	
	η=5 W/kg	η=10 W/kg	η=5 W/kg	η=10 W/kg	η=5 W/kg	η=10 W/kg
m_p [kg]	213	213	213	213	213	213
m_{th} [kg]	13.75	13.75	13.75	13.75	13.75	13.75
m_P [kg]	100	50	100	50	100	50
m_s [kg]	244.4	287.3	218.3	261.2	194.9	237.7
m_0 [kg] (with margins)	694.44	694.44	657.9	657.9	625	625

Table 3: Mass budget for missions towards the heliopause with $a_\oplus = (1.8, 1.9, 2)\,\mathrm{mm/s}^2$.

having the same time length, and performed with a square solar sail (spinning solar sail) may guarantee a payload mass fraction of 30% (40%), but requires a closer approach to the Sun at a distance of 0.25 AU, and a sailing mode time of about 5 years.

We note, in passing, that the previous mass breakdown is conservative because the power needed by the electric sail, and therefore the mass m_P, was found by neglecting the power generation system of the platform. Actually the platform RTGs, capable of providing about 240 W at the beginning of their life [7], could be used in a redundancy mode during the sailing mode time, in the interval $t \in [t_0,\, t_c]$.

Using an additional safety margin of 20% [7], from Table 3 the IHP sailcraft launch mass with electric sail option is between 750 kg and 834 kg, a value much less than the launch mass capability of the Soyouz-Fregat 2-1B, equal to 2000 kg (assuming an Earth escape with $C_3 = 0$). In particular, the solution with a Soyouz-Fregat 2-1B is identical to that conjectured for a mission scenario with a solar sail [7].

Conclusions

Missions towards the boundaries of the Solar System have been studied for an electric sail, a spacecraft that uses the solar wind dynamic pressure for generating a continuous thrust without the need for reaction mass. Assuming a two-dimensional problem in which

the orbital plane coincides with the ecliptic plane, minimum time trajectories to reach a given solar distance have been studied in an optimal framework using an indirect approach. The optimal trajectory may include or not a solar wind assist phase depending on the value of the sail characteristic acceleration. It is shown that the superiority of a direct transfer (that is, a trajectory that does not exploit the solar flyby) is confined to distances less than about 13 AU from the Sun. Once the escape condition is met, the sail is jettisoned and the payload continues its mission using a flight by inertia. A medium performance electric sail may reach a distance of 100 AU in about fifteen years.

From the obtained results, the electric sail appears as an intriguing advanced propulsion system and a promising alternative to a solar sail. Moreover, it represents a realistic option for a complex and long term mission such as the IHP mission. Of course, the practical employment of this propulsion system requires the overcoming of a number of complex challenges, such as the deployment and control of one hundred of about 20 km long tethers. The previous simplified analysis of sailcraft mass budget has shown that the structure mass must remain below 300 kg to guarantee the fulfilment of the requirement concerning the value of sailcraft characteristic acceleration. However, the wide margin used in the analysis (equal to 40% for the structure mass) offers a reasonable trust that the structure mass constraint may be met.

Finally, note that in our analysis the electric sail is used as a propulsion system external to the spacecraft platform. Such a choice is dictated by the need to obtain a reasonable comparison with the solar sail based solution, whose study is available in the literature. However, assuming to integrate the payload suite (whose mass is 20 kg only) within the electric sail and to redesign the whole power generation system in such a way to meet the sailcraft constraints during both the sailing mode time and the scientific mode, it would be possible to significantly reduce the in-flight total mass m_0 for a given value of $a_\oplus$. Clearly, this

solution requires the presence of a suitable system for tethers release that must be engaged at the instant t_c. The detailed study of this solution, which is beyond the scope of this work, can be done when a detailed mass budget model of the various subsystems of the electric sail and a more refined model for the propelling thrust will be available.

Appendix: Mathematical Model

The heliocentric equations of motion for an electric sailcraft in a polar inertial frame $\mathcal{T}_\odot(r, \theta)$ are [22]:

$$\dot{r} = u \tag{17}$$

$$\dot{\theta} = \frac{v}{r} \tag{18}$$

$$\dot{u} = \frac{v^2}{r} - \frac{\mu_\odot}{r^2} + a_\oplus \, \tau \, \cos\alpha \, \left(\frac{r_\oplus}{r}\right)^{7/6} \tag{19}$$

$$\dot{v} = -\frac{u\,v}{r} + a_\oplus \, \tau \, \sin\alpha \, \left(\frac{r_\oplus}{r}\right)^{7/6} \tag{20}$$

The Hamiltonian function associated to the maximization of the performance index (1) is

$$H = \lambda_r \, u + \lambda_\theta \, \frac{v}{r} + \lambda_u \left(\frac{v^2}{r} - \frac{\mu_\odot}{r^2}\right) - \lambda_v \, \frac{u\,v}{r} + a_\oplus \, \tau \, (\lambda_u \, \cos\alpha + \lambda_v \, \sin\alpha) \left(\frac{r_\oplus}{r}\right)^{7/6} \tag{21}$$

where λ_r, λ_θ, λ_u and λ_v are the adjoint variables associated with the state variables r, θ, u and v, respectively. The corresponding Euler-Lagrange equations are [22]:

$$\dot{\lambda}_r = \frac{\lambda_\theta\, v}{r^2} + \lambda_u \left(\frac{v^2}{r^2} - \frac{2\,\mu_\odot}{r^3} \right) - \lambda_v \frac{u\,v}{r^2} + \frac{7\,a_\oplus\,\tau}{6\,r}\, (\lambda_u\, \cos\alpha + \lambda_v\, \sin\alpha) \left(\frac{r_\oplus}{r} \right)^{7/6} \tag{22}$$

$$\dot{\lambda}_\theta = 0 \tag{23}$$

$$\dot{\lambda}_u = -\lambda_r + \lambda_v \frac{v}{r} \tag{24}$$

$$\dot{\lambda}_v = -\frac{\lambda_\theta}{r} - 2\frac{\lambda_u\, v}{r} + \frac{\lambda_v\, u}{r} \tag{25}$$

The optimal law for the control variables α and τ is [22]:

$$\alpha = \begin{cases} \operatorname{sign}(\lambda_v)\, \alpha_\lambda & \text{if} \quad \alpha_\lambda \leq \alpha_{\max} \\[2ex] \operatorname{sign}(\lambda_v)\, \alpha_{\max} & \text{if} \quad \alpha_\lambda > \alpha_{\max} \end{cases} \quad \text{with} \quad \alpha_\lambda \triangleq \arccos\left(\frac{\lambda_u}{\sqrt{\lambda_u^2 + \lambda_v^2}} \right) \tag{26}$$

$$\tau = \frac{1 + \operatorname{sign}(\lambda_u\, \cos\alpha + \lambda_v\, \sin\alpha)}{2} \tag{27}$$

where $\operatorname{sign}(\cdot)$ is the signum function and $\alpha_\lambda \in [0, \pi]$ is the Lawden's primer vector cone angle [49].

References

[1] Stone, E. C., Cummings, A. C., McDonald, F. B., Heikkila, B. C., Lal, N., and Webber, W. R., "Voyager 1 Explores the Termination Shock Region and the Heliosheath Beyond," *Science*, Vol. 309, No. 5743, September 2005, pp. 2017–2020.

[2] Richardson, J. D., Kasper, J. C., Wang, C., Belcher, J. W., and Lazarus, A. J., "Cool Heliosheath Plasma and Deceleration of the Upstream Solar Wind at the Termination Shock," *Nature*, Vol. 454, No. 7200, July 2008, pp. 63–66.

[3] Mewaldt, R. A., Kangas, J., Kerridge, S. J., and Neugebauer, M., "A Small Interstellar

Probe to the Heliospheric Boundary and Interstellar Space," *Acta Astronautica*, Vol. 35, No. Suppl., 1995, pp. 267–276.

[4] Sauer, Jr., C. G., "Solar Sail Trajectories for Solar Polar and Interstellar Probe Missions," *AAS/AIAA Astrodynamics Specialist Conference*, AAS Paper 99-336, August 1999.

[5] Dachwald, B., "Optimal Solar Sail Trajectories for Missions to the Outer Solar System," *Journal of Guidance, Control, and Dynamics*, Vol. 28, No. 6, November–December 2005, pp. 1187–1193.

[6] Falkner, P., van de Berg, M. L., Renton, D., Atzei, A., Lyngvi, A., and Peacock, A., "Update on ESA's Technology Reference Studies," 56th International Astronautical Congress, Fukuoka, Japan, 2005, Paper IAC-05-A3.2A.07.

[7] Lyngvi, A. E., van den Berg, M. L., and Falkner, P., "Study Overview of the Interstellar Heliopause Probe," Tech. Rep. 3 (revision 4), ESA, 17 April 2007, reference: SCI-A/2006/114/IHP.

[8] Dachwald, B., Macdonald, M., McInnes, C. R., Mengali, G., and Quarta, A. A., "Impact of Optical Degradation on Solar Sail Mission Performance," *Journal of Spacecraft and Rockets*, Vol. 44, No. 4, July–August 2007, pp. 740–749.

[9] Dachwald, B., Mengali, G., Quarta, A. A., and Macdonald, M., "Parametric Model and Optimal Control of Solar Sails with Optical Degradation," *Journal of Guidance, Control, and Dynamics*, Vol. 29, No. 5, September–October 2006, pp. 1170–1178.

[10] Dachwald, B., Baturkin, V., Coverstone, V. L., Diedrich, B., Garbe, G. P., Görlich, M., Leipold, M., Lura, F., Macdonald, M., McInnes, C. R., Mengali, G., Quarta, A. A., Rios-Reyes, L., Scheeres, D. J., Seboldt, W., and Wie, B., "Potential Effects of Optical Solar Sail Degradation on Trajectory Design," *AAS/AIAA Astrodynamics Specialist Conference*, AAS Paper 05–413, Lake Tahoe, CA, August 2005.

[11] Dachwald, B., Seboldt, W., Macdonald, M., Mengali, G., Quarta, A. A., McInnes, C. R., Rios-Reyes, L., Scheeres, D. J., Wie, B., Görlich, M., Lura, F., Diedrich, B., Baturkin, V., Coverstone, V. L., Leipold, M., and Garbe, G. P., "Potential Solar Sail Degradation Effects on Trajectory and Attitude Control," *AIAA Guidance, Navigation, and Control Conference and Exhibit*, AIAA Paper 2005–6172, San Francisco, CA, August 2005.

[12] McInnes, C. R., "Delivering Fast and Capable Missions to the Outer Solar System," *Advances in Space Research*, Vol. 34, No. 1, 2004, pp. 184–191.

[13] Dachwald, B., "Solar Sail Performance Requirements for Missions to the Outer Solar System and Beyond," 55th *International Astronautical Congress*, Paper IAC–04–S.P.11, Vancouver, Canada, 04–08 October 2004.

[14] Leipold, M. and Wagner, O., "'Solar Photonic Assist' Trajectory Design for Solar Sail Mis-

sions to the Outer Solar System and Beyond," *Spaceflight Dynamics 1998, Volume 100 Part 1, Advances in Astronautical Sciences*, edited by T. H. Stengle, AAS/GSFC International Symposium on Space Flight Dynamics, Greenbelt, Maryland, May, 11–15 1998, Paper AAS 98-386.

[15] Winglee, R. M., Euripides, P., Ziemba, T., Slough, J., and Giersch, L., "Simulation of Mini-Magnetospheric Plasma Propulsion (M2P2) Interacting with an External Plasma Wind," *39th Joint Propulsion Conference and Exhibition*, AIAA Paper 2003-5225, Huntsville, July 2003.

[16] Winglee, R. M., Slough, J., Ziemba, T., and Goodson, A., "Mini-Magnetospheric Plasma Propulsion: Tapping the Energy of the Solar Wind for Spacecraft Propulsion," *Journal of Geophysical Research*, Vol. 105, No. A9, 2000, pp. 21,067–21,078.

[17] Mengali, G. and Quarta, A. A., "Optimal Missions with Minimagnetospheric Plasma Propulsion," *Journal of Guidance, Control, and Dynamics*, Vol. 29, No. 1, January–February 2006, pp. 209–212.

[18] Mengali, G. and Quarta, A. A., "Minimagnetospheric Plasma Propulsion for Outer Planet Missions," *Journal of Guidance, Control, and Dynamics*, Vol. 29, No. 5, September–October 2006, pp. 1239–1242.

[19] Janhunen, P., "Electric Sail for Spacecraft Propulsion," *Journal of Propulsion and Power*, Vol. 20, No. 4, 2004, pp. 763–764.

[20] Janhunen, P. and Sandroos, A., "Simulation Study of Solar Wind Push on a Charged Wire: Basis of Solar Wind Electric Sail Propulsion," *Annales Geophysicae*, Vol. 25, No. 3, 2007, pp. 755–767.

[21] Janhunen, P., "On the feasibility of a negative polarity electric sail," *Annales Geophysicae*, Vol. 27, No. 4, 2009, pp. 1439–1447.

[22] Mengali, G., Quarta, A. A., and Janhunen, P., "Electric Sail Performance Analysis," *Journal of Spacecraft and Rockets*, Vol. 45, No. 1, January–February 2008, pp. 122–129.

[23] Mengali, G., Quarta, A. A., and Janhunen, P., "Considerations of Electric Sailcraft Trajectory Design," *Journal of the British Interplanetary Society*, Vol. 61, August 2008, pp. 326–329.

[24] Mengali, G. and Quarta, A. A., "Non-Keplerian Orbits for Electric Sails," *Celestial Mechanics and Dynamical Astronomy*, 2009, in press, doi: 10.1007/s10569-009-9200-y.

[25] Janhunen, P., Mengali, G., and Quarta, A. A., "Electric Sail Propulsion Modeling and Mission Analysis," 30th International Electric Propulsion Conference, Florence, Italy, September 17–20 2007, Paper IEPC-2007-352.

[26] Vulpetti, G., "Sailcraft at High Speed by Orbital Angular Momentum Reversal," *Acta Astronautica*, Vol. 40, No. 10, May 1997, pp. 733–758.

[27] Wallace, R. A., Ayon, J. A., and Sprague, G. A., "Interstellar Probe Mission/System Concept," *Aerospace Conference Proceedings, 2000 IEEE*, Vol. 7, Paper no. 53, Big Sky, MT, March 2000, pp. 385–396.

[28] Bryson, A. E. and Ho, Y. C., *Applied Optimal Control*, chap. 2, Hemisphere Publishing Corporation, New York, NY, 1975, pp. 71–89.

[29] Lappas, V., Leipold, M., Lyngvi, A., Falkner, P., Fichtner, H., and Kraft, S., "Interstellar Heliopause Probe: System Design of a Solar Sail Mission to 200 AU," *AIAA Guidance, Navigation, and Control Conference and Exhibit*, AIAA Paper 2005–6084, San Francisco, CA, August 15–18 2005.

[30] Leipold, M., Fichtner, H., Heber, B., Groepper, P., Lascar, S., Burger, F., Eiden, M., Niederstadt, T., Sickinger, C., Herbeck, L., Dachwald, B., and Seboldt, W., "Heliopause Explorer – a Sailcraft Mission to the Outer Boundaries of the Solar System," *Acta Astronautica*, Vol. 59, No. 8–11, October–December 2006, pp. 785–796.

[31] Leipold, M., "To the Sun and Pluto with Solar Sails and Micro-Sciencecraft," *Acta Astronautica*, Vol. 45, No. 4, August 1999, pp. 549–555.

[32] Mengali, G. and Quarta, A. A., "Optimal Three-Dimensional Interplanetary Rendezvous Using Nonideal Solar Sail," *Journal of Guidance, Control, and Dynamics*, Vol. 28, No. 1, January–February 2005, pp. 173–177.

[33] Mengali, G., Quarta, A. A., Circi, C., and Dachwald, B., "Refined Solar Sail Force Model with Mission Application," *Journal of Guidance, Control, and Dynamics*, Vol. 30, No. 2, March–April 2007, pp. 512–520.

[34] Bate, R. R., Mueller, D. D., and White, J. E., *Fundamentals of Astrodynamics*, Dover Publications, New York, 1971, p. 429.

[35] Shampine, L. F. and Gordon, M. K., *Computer Solution of Ordinary Differential Equations: The Initial Value Problem*, chap. 10, W. H. Freeman, San Francisco, 1975.

[36] Shampine, L. F. and Reichelt, M. W., "The MATLAB ODE Suite," *SIAM Journal on Scientific Computing*, Vol. 18, No. 1, January 1997, pp. 1–22.

[37] Sharma, D. N. and Scheeres, D. J., "Solar System Escape Trajectories Using Solar Sails," *Journal of Spacecraft and Rockets*, Vol. 41, No. 4, July-August 2004, pp. 684–687.

[38] Macdonald, M. and McInnes, C. R., "Analytical Control Laws for Planet-Centered Solar Sailing," *Journal of Guidance, Control, and Dynamics*, Vol. 28, No. 5, September-October 2005, pp. 1038–1048.

[39] McInnes, C. R., Dachwald, B., and Macdonald, M., "Heliocentric Solar Sail Orbit Transfers with Locally Optimal Control Laws," *Journal of Spacecraft and Rockets*, Vol. 44, No. 1, January-February 2007, pp. 273–276.

[40] Mengali, G. and Quarta, A. A., "Near-Optimal Solar-Sail Orbit-Raising from Low Earth Orbit," *Journal of Spacecraft and Rockets*, Vol. 42, No. 5, September–October 2005, pp. 954–958.

[41] Mengali, G. and Quarta, A. A., "Earth Escape by Ideal Sail and Solar-Photon Thrustor Spacecraft," *Journal of Guidance, Control, and Dynamics*, Vol. 27, No. 6, November–December 2004, pp. 1105–1108.

[42] Janhunen, P., "Status Report of the Electric Sail - A Revolutionary Near-Term Propulsion Technique in the Solar System," Sixth IAA Symposium on Realistic Near-Term Advanced Scientific Space Missions, Aosta, Italy, July 6-9 2009.

[43] McInnes, C. R., *Solar Sailing: Technology, Dynamics and Mission Applications*, Springer-Praxis Series in Space Science and Technology, Springer-Verlag, Berlin, 1999, pp. 175–196.

[44] Wright, J. L., *Space Sailing*, Gordon and Breach Science Publisher, Berlin, 1992, pp. 223–226.

[45] Mengali, G. and Quarta, A. A., "Optimal Control Laws for Axially Symmetric Solar Sails," *Journal of Spacecraft and Rockets*, Vol. 42, No. 6, November–December 2005, pp. 1130–1133.

[46] Lyngvi, A., Falkner, P., Kemble, S., Leipold, M., and Peacock, A., "The Interstellar Heliopause Probe," *Acta Astronautica*, Vol. 57, April 2005, pp. 104–111.

[47] Janhunen, P., "Increased electric sail thrust through removal of trapped shielding electrons by orbit chaotisation due to spacecraft body," *Annales Geophysicae*, Vol. 27, No. 8, 2009, pp. 3089–3100.

[48] Hunt, M. E., "High Efficiency Dynamic Radioisotope Power System for Space Exploration - A Status Report," *IEE AES System Magazine*, Vol. 8, No. 12, 1993, pp. 18–23.

[49] Lawden, D. F., *Optimal Trajectories for Space Navigation*, Butterworths, London, 1963, pp. 54–68.